

# Fall Criteria and Balance Control of Legged Robots: Literature Review and Analysis

## Gait and Manipulation

Manthan Pawar  
 New York University  
 Tandon School of Engineering  
 Brooklyn, New York  
 Mvp321@nyu.edu

**Abstract-** This a report on Fall Criteria and Balance Control of Legged Robots: Literature Review and Analysis submitted towards the final submission for the gait and manipulation course under the guidance of professor J. H. Kim, New York University, Tandon School of Engineering. The project covers Balance stability criteria: Existing fall criteria used in the current legged robots. In particular, the threshold of “fall” that triggers the balancing action during, e.g., push recovery, walking and Balance stability control methods used to following the fall detection. Legged robots include humanoids, exoskeletons, quadrupeds, etc.

The report classifies the criteria and control methods according to similarities and types.

**Index Terms-** Legged Robots, gait and manipulation, stability criteria, threshold, Balance stability control.

## I. IMPORTANT TERMS

**Fall Criteria:** Fall criteria is the phenomenon used for the legged robots using which it is determined that if the robot is in falling state of stable state.

**Threshold:** A threshold is a condition of physical parameters of the biped robots that defines the border between falling state and the stable state of the robot.

**Control Policy:** Control Policy is a methodology used to compensate for the instability of legged robots that regains the balance of the legged robot and do not let it fall.

## II. PAPER NOTES

**1) Principles of robot locomotion, Sven Böttcher, Proceedings of human robot interaction seminar, 2006.**  
 [Böttcher, Sven. “Principles of robot locomotion.” (2006).]

1. The **support polygon** is the convex hull which is set by the ground contact points.
2. **Static stability** is given, when the center of mass is completely within the support polygon and the polygon’s

area is greater than zero, therefore static stability requires at least three points of ground contact.

3. Biped Robots must be Dynamically stabilized.
4. To achieve statically stable walking a robot must have a minimum number of four legs, because during walking at least one leg is in the air.
5. robots’ center of mass must be shifted actively between the footprints
6. robots exact center of mass is hard to predict due to the high dynamic of walking
7. adding degrees of freedom to a robot’s leg means **increasing the maneuverability** of the robot, the range of terrain on which it can travel and the ability to travel in a variety of gaits.
- Two-Legged Robot:
8. The ZMP is the point where the robot has to base on to keep its balance.

$$(1) \quad x_{ZMP} = \frac{\sum_i m_i(z+g)x_i - \sum_i m_i x z_i - \sum_i I_{iy}\theta_y}{\sum_i m_i(z+g)}$$

$$(2) \quad y_{ZMP} = \frac{\sum_i m_i(z+g)y_i - \sum_i m_i y z_i - \sum_i I_{ix}\theta_x}{\sum_i m_i(z+g)}$$

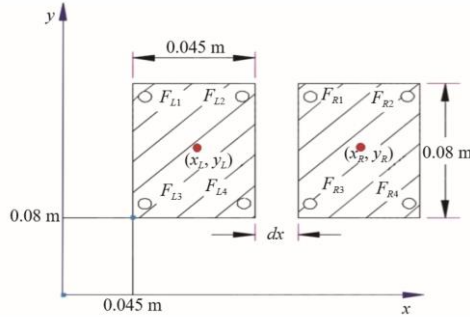
9. To support stability the ZMP has to be completely within the support polygon.
10. If one leg is in the air, the support polygon is equal to the shape of the foot which relates to the ground, so the ZMP has to be completely within the footprint to support stability.

**2) Balance Control of a Biped Robot on a Rotating Platform Based on Efficient Reinforcement Learning**

[A. Xi, T. W. Mudiyanselage, D. Tao and C. Chen, "Balance control of a biped robot on a rotating platform based on efficient reinforcement learning," in IEEE/CAA Journal of Automatica Sinica, vol. 6, no. 4, pp. 938-951, July 2019.]

**Robot:** NAO robot on a rotating platform

Used Inverted pendulum Model to simulate the system  
No knee joints in simulation  
**Fall criteria:** COP



$$Y = \frac{y_1 F_1 + y_2 F_2 + y_3 F_3 + y_4 F_4}{F_1 + F_2 + F_3 + F_4} \quad (1)$$

where  $y_i$  denotes the  $y$  coordinates for the foot sensors, whereas  $F_i$  is the corresponding pressure read from the sensor. As a result, the position of CoP for the two feet can be computed as

$$Y_{\text{CoP}} = Y_L \left( \frac{F_L}{F_L + F_R} \right) + (Y_R + d_Y) \left( \frac{F_R}{F_L + F_R} \right) \quad (2)$$

**Threshold:** During the procedure of collecting training data for the first layer GP, the robot fails if the CoP is located without the region of  $y$  [0.08, 0.16]. Therefore, the stable region is consequently defined, and the target state is also defined as  $y_0 = 0.116$  m. The robot can maintain its standing posture vertical to the ground if the CoP is exactly located at  $y_0 = 0.116$  m

**Control Policy:** model-based reinforcement learning (MBRL)

Markov decision process (MDP): In the reinforcement learning, an agent (robot) takes an action according to the learned policy, where the policy is generated and updated during the interaction with the environment [31]. The interaction between the robot and the environment can be described as a Markov decision process (MDP) - which can be presented as a tuple.  $S$  is the state space that describes the dynamic of the robot.  $A$  is the action space.  $\pi$  is the probability of transition to a future state  $s_{t+1}$  when the robot is in current state  $s_t$  and applied an action  $a_t$ .

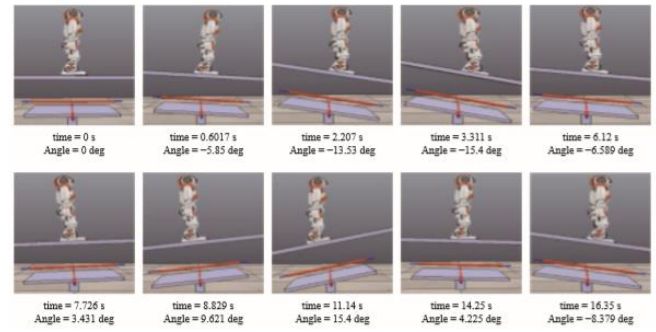
$s_{t+1}$  after applying action  $a_t$ . The objective of RL is to find a policy that minimizes the following expected long term cost

$$Q(s_t, a_t) = E \left[ \sum_{t=0}^T [C(s_t, a_t)] \right] = \sum_{t=0}^T E [C(s_t, a_t)] \quad (3)$$

$Q(s_t)$  is called action value function. Here, the policy can be considered as a sequence of actions  $\pi(s_0) \rightarrow (a_0, a_1, a_2, \dots, a_T)$ . As a result, the actions for each state can be selected using greedy algorithm that minimizes the expected immediate cost at this state

$$a_t = \underset{a \in A}{\operatorname{argmin}} Q(s_t, a_t). \quad (4)$$

Gaussian Processes and Optimization



8. Screenshots of the experiment.

### 3) Balancing Stability and Maneuverability during Rapid Gait Termination in Fast Biped Robots

[S. Shield and A. Patel, "Balancing stability and maneuverability during rapid gait termination in fast biped robots," 2017 IEEE/RSJ International Conference on Intelligent Robots and Systems (IROS), Vancouver, BC, 2017, pp. 4523-4530.]

**Robot:** 7 DOF bipedal Model

Stability in rapid gait

ZRAM:

stopping distance could be reduced by 12% and time by 25% by relaxing the ZRAM condition, with greater reductions possible through the addition of a free stabilizing limb.

The ability to moderate the pitch of the robot while decelerating was found to be paramount to achieving a rapid stop and thus, a template incorporating an inertial body and stabilizing appendages is proposed to represent these maneuvers. The paper talks about the previous findings of stability criteria

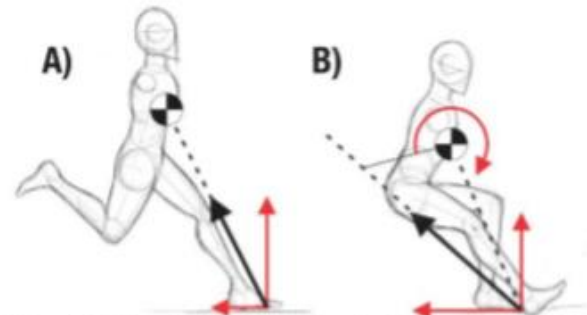


Figure 1: When the GRF line of action intersects the COM, no moment is produced and the robot remains stable (left). During deceleration, however, the large rearward GRF tends to induce a toppling moment (right).

#### Previous work for stability of The Robot in motion:

Criteria and threshold author talk about: The robot is stable if the rate of change in angular momentum at each instant is zero (ZRAM). Means, GRF passes through COM.

## Fall Criteria and Balance Control of Legged Robots: Literature Review and Analysis

**Control Policy:** This is achieved by placing the foot such that the line of action of the GRF intersects the center of mass (COM)

### The robot in deceleration:

large rearward GRF tends to induce a toppling moment (right).

### Model:

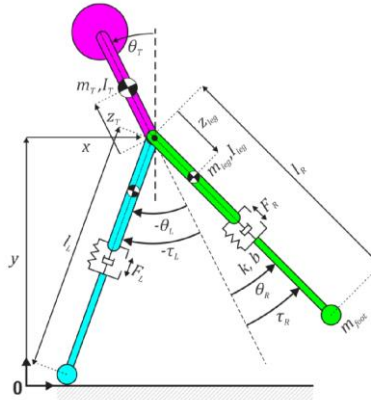


Figure 2: Seven degree-of-freedom bipedal model.

$$\mathbf{q} = [x, y, \theta_T, \theta_R, \theta_L, l_R, l_L]^T$$

$$\mathbf{u} = [F_R, F_L, \tau_R, \tau_L]$$

### Threshold:

stopping is defined as

$$\dot{x}_{CN} = 0$$

$$\dot{\theta}_{TN} = 0$$

$$G_{xR_N} + G_{xL_N} = 0$$

$$\dot{H}_N = 0$$

$$y_{FootR_N} = y_{FootL_N} = 0$$

where  $\dot{x}_C$  is the horizontal velocity of the COM,  $G_{xR}$  and  $G_{xL}$  are the horizontal ground reaction forces at the right and left feet, and  $y_{FootR}$  and  $y_{FootL}$  are the heights of the feet. The change in angular momentum,  $\dot{H}$ , represents the net torque acting on the system [11]. Condition (7.5) forces the model to finish with both feet on the ground.

### Cost Function:

In these experiments, 'rapid' refers to the minimization of the distance and time over which the stopping manoeuvre is completed. This can be translated to the following cost function:

$$J = \sum_{i=0}^N (h_i^2 \dot{x}_i^2 + \rho \cdot p_i) \quad (8)$$

### Result:

Impact of ZRAM condition on rapid deceleration

The stopping distances and times for all trajectories are compared in Figure 4. Adhering to the ZRAM condition increased the stopping distance by  $(0.40 \pm 0.16)$  m, or 12.5 percent, and the stopping time by  $(0.18 \pm 0.04)$  s, or 24.7 percent.

### Control Policy:

**Leg Swing:** one leg is swung rapidly backwards. The other foot remains in front of the body and may or may not be in contact with the ground.

**Alternating stance:** the feet are both in front of the body and contact the ground one at a time.

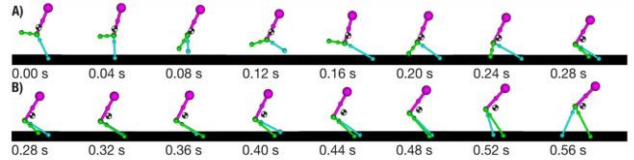


Figure 5: Animation of a stopping trajectory. A) shows the leg swing motion, where one leg is rotated rapidly backwards, thereby keeping the COM in a centric position. B) shows the alternating stance, where both feet are in front of the robot and contact the ground one at a time. This posture shifts the COM forward.

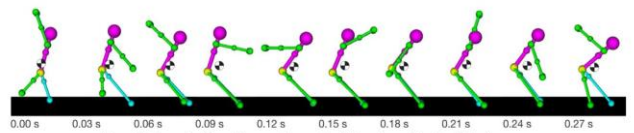


Figure 15: Example of a rapid arm-rotating motion that can be used to absorb kinetic energy.

### My View:

For previous work, we have been using  $ZRAM = 0$  criteria for bipeds where GRF passes through COM.

ZRAM takes time.

ZRAM can be relaxed by letting pitch increase.

ZRAM and Baseline consist of 2 types of stopping strategies – leg swing and alternating stance

To compensate for increased pitch, 2 Ways to relax ZRAM condition. 1) Baseline model – in which leg swing is less and alternating stance is more. 2) Stabilizing limb model – leg swing, alternating stance + limb swing

## 4) Control Design to Achieve Dynamic Walking on a Bipedal Robot with Compliance

[Bokman Lim et al., "Control design to achieve dynamic walking on a bipedal robot with compliance," 2012 IEEE International Conference on Robotics and Automation, Saint Paul, MN, 2012, pp. 79-84.]

### Introduction:

Main contribution is a development of an adaptive control framework for generating dynamic locomotion under external disturbances.

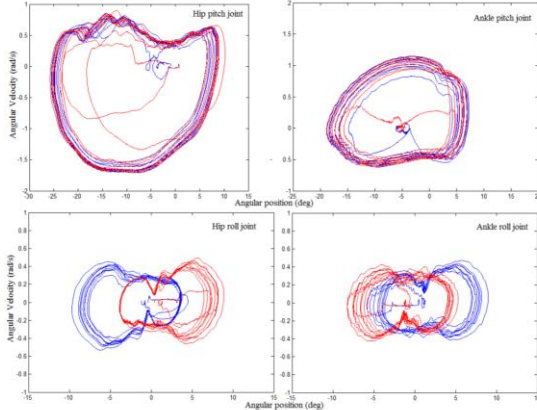
driving robot joints directly in the joint space with the posture-based state machine (notice that we do not solve inverse kinematics problem) and

controlling tendon-driven (compliant) actuator with low control gains.

**Robot:** Roboray 32 joint

**Fall Criteria:** Limit Cycle

**Threshold:**



### Controls of the Robot:

$$\tau_{des} = \omega_1 \tau_{fsm} + \omega_2 \tau_{g-comp} + \omega_3 \tau_{model} + \omega_4 \tau_{reflex} \quad (1)$$

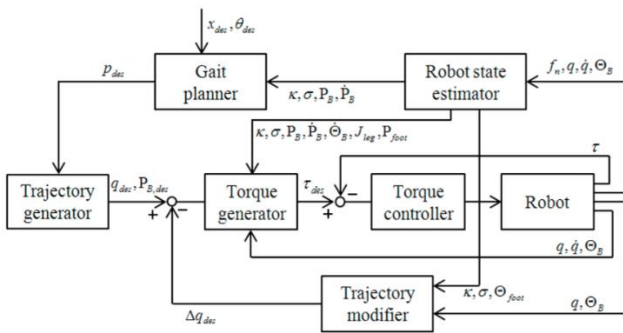
where  $\omega_1, \dots, \omega_4$  are weighting factors.

1) *State Machine based Control:* The state dependent control torque is generated by simple spring-damper couples with the desired target trajectory  $q_{des}$ .

$$\tau_{fsm} = k_p(q_{des} - q) - k_d \dot{q} \quad (5)$$

2) *Swing Leg Gravity Compensation:* Gravity compensation control makes us possible to use low control gains. For this calculation, recursive dynamics algorithm [14] is used with the current orientation of the robot base  $\Theta_B$ , desired joint angle  $q_{des}$ , zero velocity and zero acceleration. Gravity compensation torques are applied to only swing leg joints.

3) *Stance Leg Balancing with Virtual Model:* A stance leg balancer increases the gait's basin attraction for stable walking. A model based virtual 6D force  $F_{virtual}$  is generated



by the desired robot base position.

$$F_{virtual} = \begin{bmatrix} k_{p1}m(P_{B,des} - P_B) - k_{d1}m\dot{P}_B \\ -k_{d2}m\dot{\Theta}_B \end{bmatrix} \quad (6)$$

$$\tau_{model} = J_{leg}^T F_{virtual}$$

where  $k_{p1}, k_{d1}, k_{d2}$  are control gains,  $P_{B,des}$  is a desired target base position,  $P_B$  is a current base position,  $\dot{P}_B$ ,  $\dot{\Theta}_B$  are current robot base linear and angular velocities, and  $J_{leg}$  is the Jacobian from the support foot to the base.

4) *Sensory Reflex Control with Potential Barrier:* A reflex control has two main roles: 1) collision avoidance [15] between the stance leg and the swing leg, and 2) reflexive motion for sudden external disturbances. Using potential barriers we generate a repulsive hip roll torque. With a virtual model control, the reflex control is important to recover falling motion in the frontal plane.

$$\tau_{reflex} = \begin{cases} \eta \left( \frac{1}{\rho} - \frac{1}{\rho_0} \right) \frac{1}{\rho^2} & \text{if } \rho \leq \rho_0 \\ 0 & \text{if } \rho > \rho_0 \end{cases} \quad (7)$$

where  $\eta$  is the weighting factor,  $\rho_0$  is a distance limit of the influence, and  $\rho$  is a measured distance for the reflex control. In collision avoidance, we use the projected distance between the feet in the frontal plane. In reflexive balancing, we use the distance between the potential wall and the robot base in frontal plane as  $\rho = d_{max} - l_{leg} \sin(\Theta_{B,roll})$  (see Fig. 8).

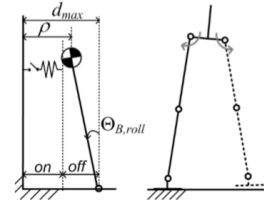


Fig. 8. An inverted pendulum model and potential barriers for reflexive balancing

### 5) Dynamics Simulation for a Biped Robot: Modeling and Experimental Verification

[T. Buschmann, S. Lohmeier, H. Ulbrich and F. Pfeiffer, "Dynamics simulation for a biped robot: modeling and experimental verification," Proceedings 2006 IEEE International Conference on Robotics and Automation, 2006. ICRA 2006., Orlando, FL, 2006, pp. 2673-2678.]

**Robot:** JOHNNIE.

## 6) Trajectory Generation of Biped Running Robot with Minimum Energy Consumption

[Y. Fujimoto, "Trajectory generation of biped running robot with minimum energy consumption," IEEE International Conference on Robotics and Automation, 2004. Proceedings. ICRA '04. 2004, New Orleans, LA, USA, 2004, pp. 3803-3808 Vol.4.]

## 7) Reflex Control of Biped Robot Locomotion on a Slippery Surface

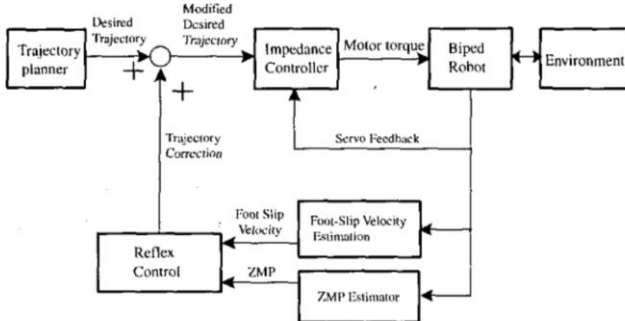
[Jong Hyeon Park and Ohung Kwon, "Reflex control of biped robot locomotion on a slippery surface," Proceedings 2001 ICRA. IEEE International Conference on Robotics and Automation (Cat. No.01CH37164), Seoul, South Korea, 2001, pp. 4134-4139 vol.4.]

**Robot:** 12 DOF biped Robot

**Fall Criteria:** ZMP

**Threshold:** When the horizontal acceleration of the foot on the ground is above a certain level, it is assumed that slipping occurs at the foot

**Controls:** e reflex control and the on-line ZMP compensation



### Introduction:

Recovery from slipping of the foot of biped robot on slippery surface with slow gait.

It is based on the reflex control and the on-line ZMP compensation.

When a robot enters a slippery area, it may change its locomotion pattern in many ways.

### Slipping Condition:

From computer simulations of locomotion of a biped robot controlled by the impedance controller, some patterns of foot slips were obtained. (controller doesn't know the surface at all).

when the impedance control [4] is applied such that the landing feet behaviors according to the desired impedance characteristics, the locomotion becomes very robust and slipping phenomena were significantly suppressed without any separate control scheme to avoid slipping.

Impedance control cannot handle high speeds.

### Reflex Control:

A quick and simple control algorithm, which imitates the reflexes of human beings.

Reflex control consists of three phases: detection of a slip at the feet, fast adaptation, and the recovery to the normal locomotion pattern

### 3 Reflex control methods:

First, the hip link of the biped robot is lifted up vertically. A positive acceleration of the hip link in the vertical direction would increase the contact force between the ground and the foot on it. As the ground reaction force at the foot becomes larger, the friction force parallel to the ground increases, stopping the slipping. This idea is implemented by changing the desired acceleration of the hip link in the vertical direction, which is normally zero.

$$\ddot{z}_0^d = c_1 \cdot |v_{slip}|$$

where V-slip is the slipping velocity of the foot and c1 is a constant gain.

shift the foot of the robot into the horizontal direction keeps the balance of the robot by moving the foot of the swinging leg into the direction for the foot of the supporting leg to slip. A shift of the swinging foot toward the supporting leg in the horizontal direction is implemented by changing the desired velocity of the slipping foot:

$$\dot{y}_f^d = c_2 \cdot |v_{slip}| \cdot (y_f^d - y_f)$$

where V-slip is the velocity of the slipping foot in the lateral direction, and  $y_f^d$  and  $y_f$  are the desired and actual lateral positions of the slipping foot, respectively.

In some other cases, the control could run out of the elevation space of the hip link or the movement space of the swing leg due to the kinematic limits in the robot joints. To cope with these situations, this paper proposes an additional reflex control algorithm based on the on-line ZMP compensation. *shift the hip link in a horizontal direction such that the ZMP of the robot moves into the safety region.*

The hip link is moved by changing its desired acceleration depending on the deviation of the ZMP from the boundary of its safety region, i.e.,

$$\ddot{x}_0^d = \ddot{x}_0 + c_3 \cdot (x_{ZMP} - x_{ZMP}^B)$$

$$\ddot{y}_0^d = \ddot{y}_0 + c_4 \cdot (y_{ZMP} - y_{ZMP}^B)$$

where  $\ddot{x}_0$  and  $\ddot{y}_0$  are the acceleration of the hip link in the walking direction and in the lateral direction, respectively;  $[x_{ZMP} \ y_{ZMP}]^T$  and  $[x_{ZMP}^B \ y_{ZMP}^B]^T$  are the ZMP position and the boundary position of the ZMP safety region that is the closest to the ZMP position, respectively.

## 8) A Machine Learning Approach to Falling Detection and Avoidance for Biped Robots

[J. Kim, Y. Kim and J. Lee, "A machine learning approach to falling detection and avoidance for biped robots," SICE Annual Conference 2011, Tokyo, 2011, pp. 562-567.]

### Robot: 6 DOF

**Fall Criteria:** Detect falling of a biped robot with Support Vector Machine (SVM). Acceleration value of the torso of the robot, force sensing resistor (FSR) value on the foot and COP data are used as input feature vector of the SVM. And the SVM classify the state of the robot based on the value.

#### Threshold:

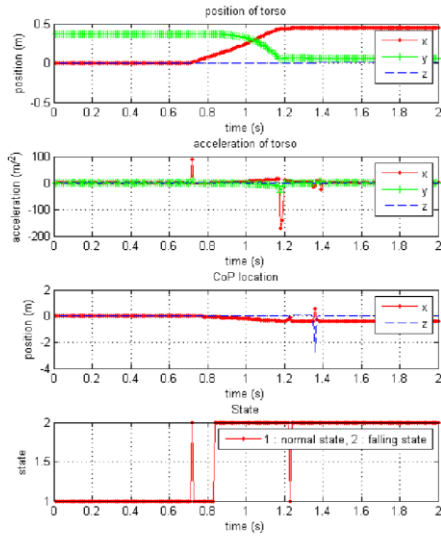


Fig. 6 Falling detection when the robot is standing and the force is applied from back.

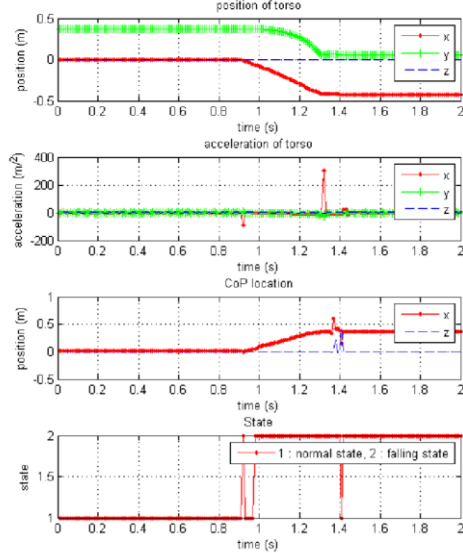


Fig. 7 Falling detection when the robot is standing and the force is applied from front.

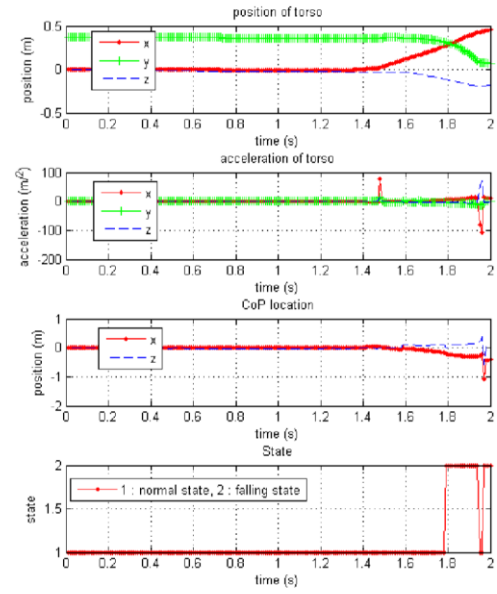


Fig. 8 Falling detection when the robot is walking and the force is applied from back.

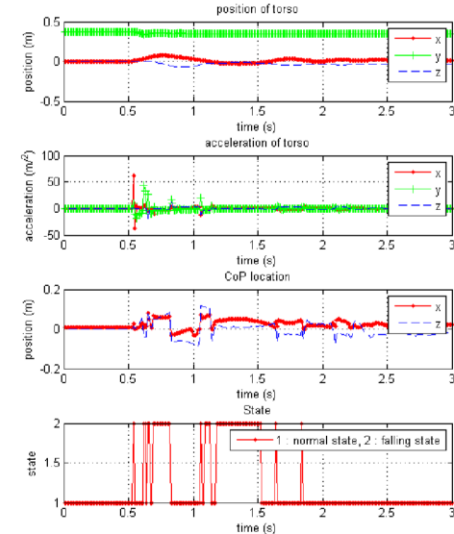


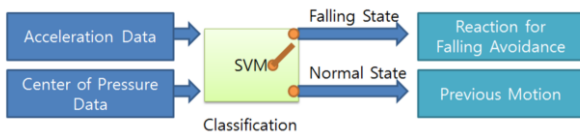
Fig. 9 Falling detection and recovery reaction when the robot is standing and the force is applied from back.

### Controls:

Increasing the support polygon area.

Reaction motions are two types, stretching leg forward and backward, and each motion is selected according to the falling direction. When the robot is falling forward, the leg located at backward is moved in front of the torso and the robot is falling backward, the leg located at forward is moved at the rear.

## Fall Criteria and Balance Control of Legged Robots: Literature Review and Analysis



### 9) Fall Detection in T-FLoW Humanoid Robot: V-REP Simulation

[M. Arfaq, R. S. Dewanto and D. Pramadihanto, "Fall Detection in T-FLoW Humanoid Robot: V-REP Simulation," 2018 International Electronics Symposium on Engineering Technology and Applications (IES-ETA), Bali, 2018, pp. 224-228.]

**Robot:** T-FloW humanoid robot

**Fall criteria:** ZMP + IMU

**Threshold:** threshold values of the z acceleration, x angular velocity, and roll angle that indicate falling condition are  $-6.9708 \text{ m/s}^2$ ,  $39.16 \text{ deg/s}$ , and  $-4.27 \text{ degrees}$ .

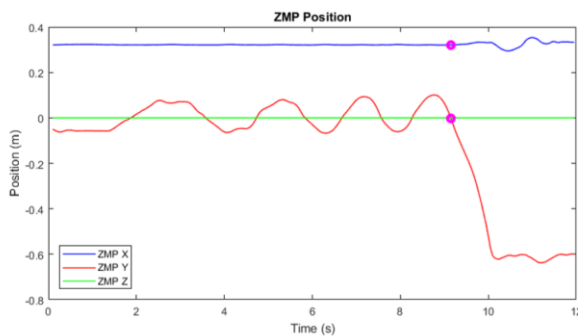


Fig. 10. Calculated ZMP position

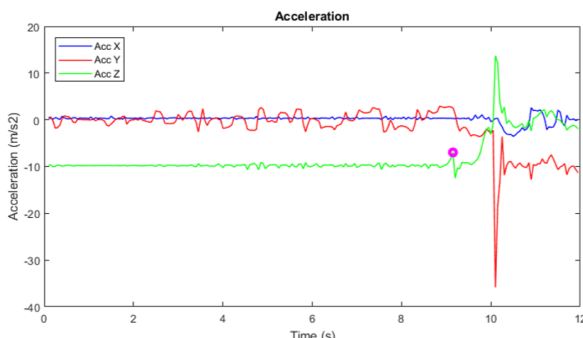


Fig. 11. Acceleration data

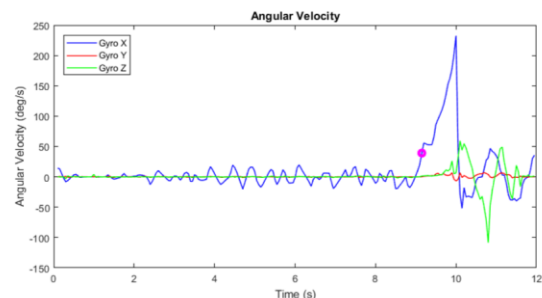


Fig. 12. Angular velocity data

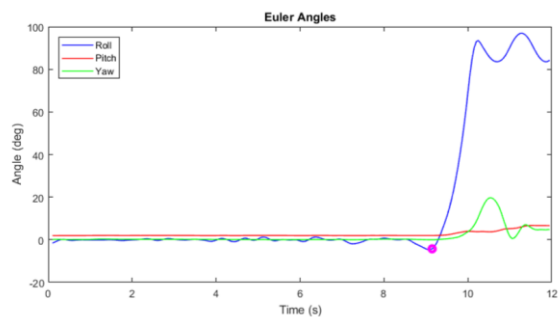
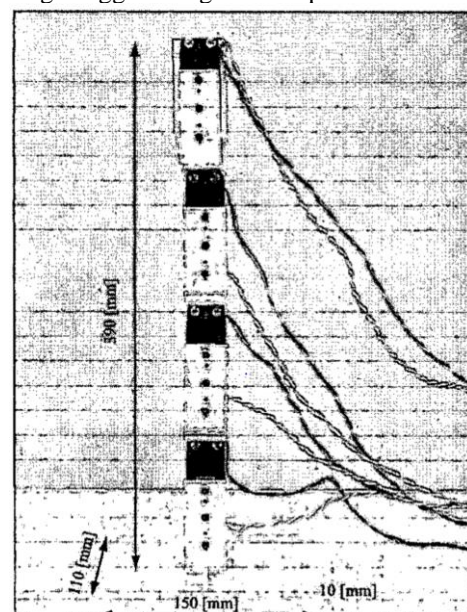


Fig. 13. Euler angles data

### 10) A Biologically Inspired CPG-ZMP Control System for the Real-time Balance of a Single-Legged Belly Dancing Robot

[J. Or and A. Takanishi, "A biologically inspired CPG-ZMP control system for the real-time balance of a single-legged belly dancing robot," 2004 IEEE/RSJ International Conference on Intelligent Robots and Systems (IROS) (IEEE Cat. No.04CH37566), Sendai, 2004, pp. 931-936 vol.1.]

**Robot:** Single legged 4 segmented spine robot



### Fall criteria: ZMP

**Threshold:** the plastic plate at the bottom of the robot serves as a foot sole. The surface area of this plate is the support polygon of the robot. When the robot is balanced, the ZMP trajectory remains within this polygon and the torque of the base motor is small. When the robot is losing its balance, the ZMP leaves the support polygon. At that instance, a high torque is generated at the base joint. By monitoring the torque at this joint, we are able to determine whether the robot is in dynamic equilibrium or not. If the torque is larger than an experimentally defined threshold value (which indicates that the robot is on the verge of falling),

**Control Policy:** If the torque is larger than an experimentally defined threshold value (which indicates that the robot is on the verge of falling), an inhibiting feedback signal is sent to the CPG to reduce the level of excitations from the brainstem. This in turn reduces the amplitude and frequency of the spine motions. Spine motions become less violent and the robot is able to belly dance stably on the floor. Consequently, the torque at the base joint motor is reduced.

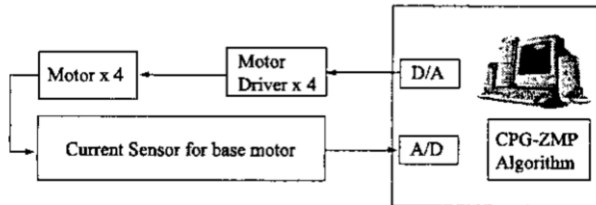
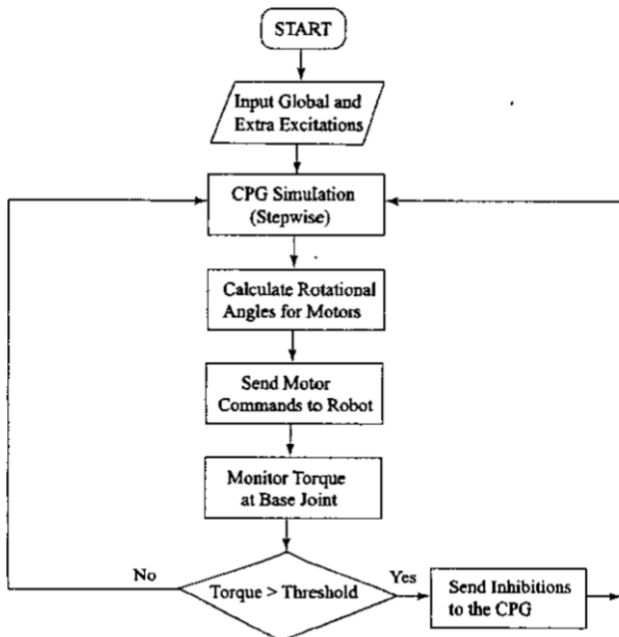


Fig. 4. Schematic diagram of the experimental setup.



### 11) Balancing a Humanoid Robot Using Back Drive Concerned Torque Control and Direct Angular Momentum Feedback

[S. Kajita, K. Yokoi, M. Saigo and K. Tanie, "Balancing a humanoid robot using backdrive concerned torque control and direct angular momentum feedback," Proceedings 2001 ICRA. IEEE International Conference on Robotics and Automation (Cat. No.01CH37164), Seoul, South Korea, 2001, pp. 3376-3382 vol.4.]

**Robot:** 26DOF humanoid robot - novel balancing control for a humanoid standing with one leg

**Fall Criteria:** (6-axis force sensor measures force and torques acting from the robot to a ground and the information can be used for balancing and walking.)

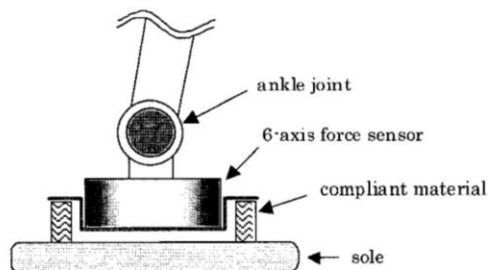


Figure 1: Foot structure with a 6-axis force sensor and passive compliance

**Threshold:** Not studied

**Control Policy:** robot controls a contact torque between the robot and the ground. By rotating the ankle joint the robot can generate the contact torque of desired magnitude.

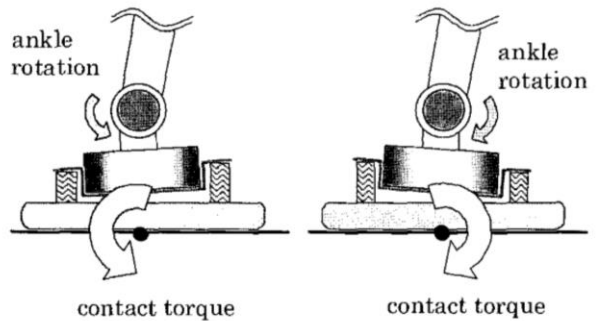


Figure 2: Left: When a robot rotates the ankle CCW with respect to the leg, it generates CCW contact torque. Right: When a robot rotates the ankle CW with respect to the leg, it generates CW contact torque.

### 12) Effect of Gravity Balancing on Biped Stability

[A. Agrawal and S. K. Agrawal, "Effect of gravity balancing on biped stability," IEEE International Conference on

## Fall Criteria and Balance Control of Legged Robots: Literature Review and Analysis

Robotics and Automation, 2004. Proceedings. ICRA '04. 2004, New Orleans, LA, USA, 2004, pp. 4228-4233 Vol.4.]

(If the ZMP lies within the convex hull of all contact points between the feet and the ground, the biped robot is dynamically stable and can sustain motion.)

Section 2 describes the theory of gravity balancing machines. Section 3 describes typical human gait cycle. Section 4 deals with kinematic and dynamic modeling of a biped system. Section 5 contains comparison of designs based on stability and torque inputs.

**Robot:** The kinematic model of the biped consists of a chain of 7 rigid bodies with 11 variables that define its motion.

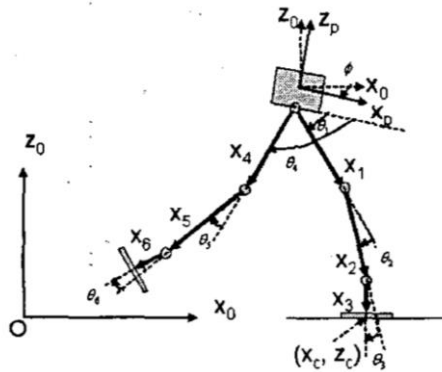


Fig. 5. Biped Kinematic Model

**Fall Criteria:** To analyze the dynamic stability of a biped robot, the zero-moment point (ZMP) criterion has been proposed

**Threshold:**

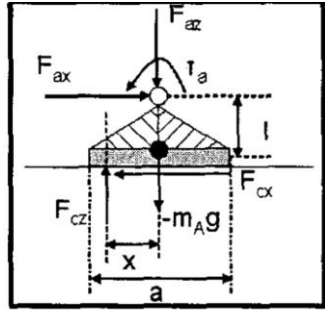


Fig. 6. Free Body Diagram of Ankle

by balancing the moment about the ankle

$$\tau_a - F_{cx}l - F_{cz}x_{zmp} = 0, \quad (19)$$

$$x_{zmp} = \frac{\tau_a - F_{cx}l}{F_{cz}}, \quad (20)$$

$$\frac{-a}{2} \leq x_{zmp} \leq \frac{a}{2}, \quad (21)$$

where  $\tau_a$  is torque input at the ankle joint,  $F_{cx}$  and  $F_{cz}$  are the ground reaction forces.

If the ZMP lies within the convex hull of all contact points between the feet and the ground, the biped robot is dynamically stable and can sustain motion.

## Control Policy:

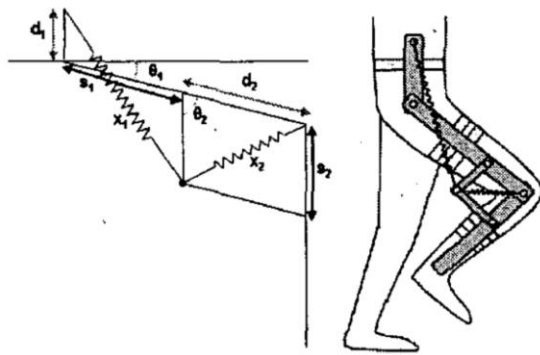


Fig. 1. Two Link System Design

The force on biped with device with spring inertially fixed is quite low compared to the biped with device without springs because of the vertical component of the spring force, which always acts in opposite direction to the gravity. Also, the vertical ground reaction force is around 700 N which is almost equal to the weight of the biped. The horizontal ground reaction force also changes because of the horizontal spring force component.

Fig. 9 shows ZMP trajectory for the two cases and we can see that in the case of biped with device and without springs ZMP lies in the foot support area while in the other case ZMP goes outside the foot and the biped is not able to maintain stability. In the second plot of Fig. 9 the factor alpha is defined as

$$\alpha = |F_{cx}| / F_{cz} \quad (26)$$

$$\text{or, } \alpha \leq \mu \quad (27)$$

In this paper, we have assumed  $\mu = 0.5$ . In general, we would expect that  $\alpha \leq 0.5$ , but from the plot  $\alpha$  becomes greater than 0.5 for the case of biped with device and spring point inertially fixed as the vertical ground reaction force drops in this case. This means that in this case the biped is not able to maintain friction conditions.

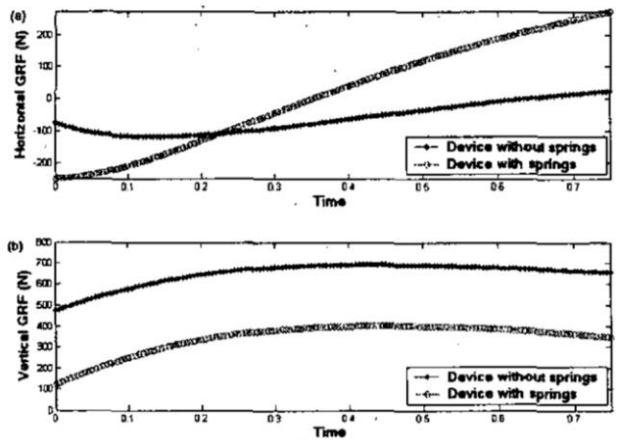


Fig. 8. Ground Reaction Forces

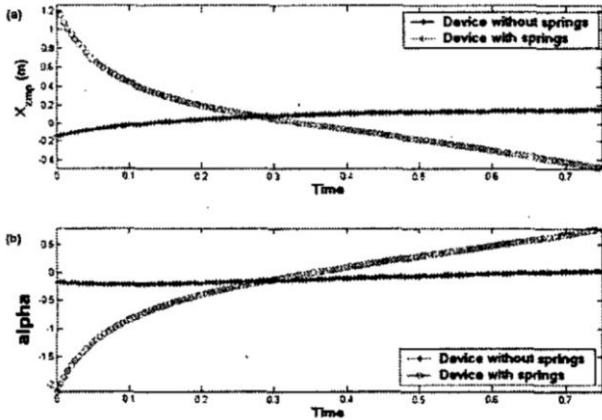


Fig. 9. ZMP Trajectory And Alpha

The results show that gravity balancing reduces the torques required at the joints of the right leg. But it affects the stability of the biped when the spring connection point is inertially fixed as it can be seen from the results that ZMP point goes out of the foot support area, and the friction conditions are also not satisfied

### 13) A Biomechanically Motivated Two-Phase Strategy for Biped Upright Balance Control

[M. Abdallah and A. Goswami, "A Biomechanically Motivated Two-Phase Strategy for Biped Upright Balance Control," Proceedings of the 2005 IEEE International Conference on Robotics and Automation, Barcelona, Spain, 2005, pp. 1996-2001.]

(The paper talks about two strategies, Reflex Phase and Recovery Phase)

**Reflex:** Quickly absorb Disturbance force- generating increase in angular momentum.

**Recovery:** Recovery of original posture- compensate for the posture deviation accepted during Reflex control.

**Robot:** Model consist of the foot, shank, thigh, and HAT. joints: the ankle, knee, and hip.

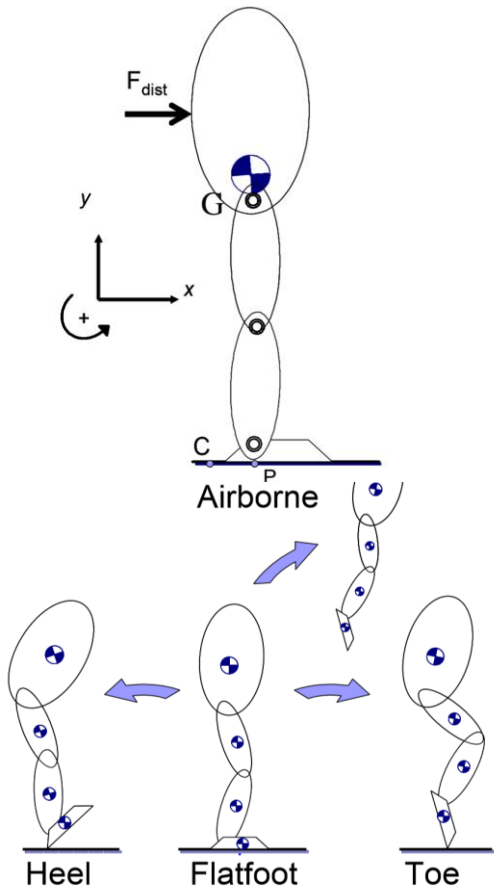


Fig. 2. A planar upright humanoid model for balance studies. The model has 4 foot-ground contact states: Flatfoot, Toe, Heel and Airborne.

**Fall Criteria:** COP - Our objective in this paper is to maintain the full controllability of the robot. We will do so by regulating the CoP to keep it in the interior of the foot, away from the edge, and thus keep the system fully actuated.

**Threshold:** The CoP must remain within the convex hull of the ground support area. As long as it is within the interior of the foot, the system has greater flexibility to withstand perturbation since the CoP can move in any direction along the ground. Once the CoP reaches the boundary, it can no longer proceed in the respective direction, losing a degree of controllability and the system becomes under-actuated.

(For a robot with a flat foot resting on a level surface, a CoP within the interior of the foot implies that the foot is stationary and flat against the ground. A CoP on the boundary indicates that the foot is either pivoting about its edge or on the verge of pivoting. For our robot model, a CoP within the interior of the foot is represented by the Flatfoot phase, while a CoP on the boundary is represented by the Toe or Heel phase respectively.)

*The key is not stability but the robot's controllability at the current state.*

**Control Policy:**

Reflex: Quickly absorb Disturbance force- generating increase in angular momentum.

Recovery: Recovery of original posture- compensate for the posture deviation accepted during Reflex control.

Reflex:

$$\mathbf{r}_{cp} = \frac{\mathbf{n} \times (\dot{\mathbf{H}}_G + \mathbf{r}_{CG} \times m(\mathbf{a}_G - \mathbf{g}) - \mathbf{r}_{CF} \times \mathbf{F})}{\mathbf{n} \cdot \mathbf{R}} \quad (2)$$

where  $\mathbf{r}_{cp}$  is the position vector from C to CoP,  $\mathbf{n}$  is the ground normal,  $\dot{\mathbf{H}}_G$  is the time-derivative of the angular momentum about the center of mass (CoM),  $\mathbf{r}_{CG}$  is the vector from C to the CoM,  $m$  is the total mass of the robot,  $\mathbf{a}_G$  is the CoM acceleration,  $\mathbf{F}$  is the net “non-ground” external forces,  $\mathbf{r}_{CF}$  is the vector from C to the point of application of  $\mathbf{F}$ , and  $\mathbf{R}$  is the GRF.

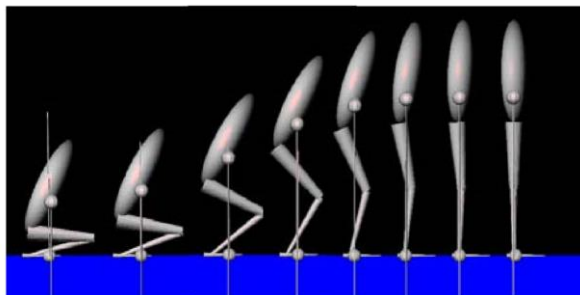
If we apply this equation to our planar robot standing on a horizontal surface and under a horizontal disturbance force  $\mathbf{F}_{dist}$  as shown in Fig. 3, we obtain the following equation:

$$\begin{aligned} x_p &= \frac{mg}{d} x_G + \frac{\dot{H}_c}{d} + \frac{y_F F_{dist}}{d} \\ d &= \dot{L}_y + mg \end{aligned} \quad (3)$$

where  $x_p$  is the x-coordinate of the CoP,  $x_G$  is the x-coordinate of the CoM,  $\dot{H}_c$  is the time-derivative of the angular momentum about point C, and  $\dot{L}_y$  is the y-component of the time-derivative of linear momentum. Note

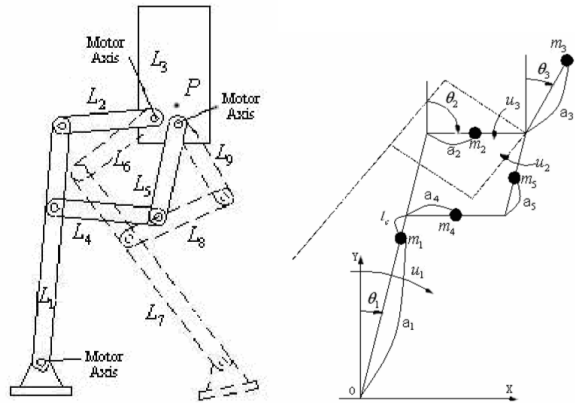
The middle term of this equation represents the “falling forward” term that is used to absorb the disturbance. It now allows us to isolate the component that moves the CoM horizontally,  $L_x$ . Due to the redundancy in our system, we can control the angular and the linear momentum independently. We can now use  $\dot{H}_c$  to absorb the disturbance while regulating  $\dot{L}_x$  to limit the CoM forward motion. The next section contains the models used to control momenta.

Recovery: The posture which has the highest PE.

**14) Gait Design and Balance Control for the Biped Robot Based on Reaction Null space Method\***

[H. Chuangfeng, F. Yuefa and G. Sheng, "Gait Design and Balance Control for the Biped Robot Based on Reaction

Null-space Method," 2007 Chinese Control Conference, Hunan, 2007, pp. 169-173.]

**Robot:**

(a) System link structure (b) Mechanics model

Fig.1 Biped system model

We introduce the reaction null-space method and will use a 6-DOF biped robot model. The whole biped sys-

**Fall Criteria: ZMP****15) Design and Implementation of a Closed-Loop Static Balance System for the YICAL Leg 2 Biped**

[F. J. O. Corpuz, B. C. Y. Lafoteza, R. A. L. Broas and M. Ramos, "Design and implementation of a closed-loop static balance system for the YICAL Leg 2 biped," TENCON 2009 - 2009 IEEE Region 10 Conference, Singapore, 2009, pp. 1-6.]

In the system, an attitude estimation system was developed to detect changes in the tilt and rotation along the hip axis of the biped. The attitude estimation system utilized an accelerometer and a rate gyroscope. Based on the information obtained from the attitude estimation system, the Balancing and Position Control Algorithms were programmed to execute reflex motions to counter instabilities applied to the bipedal robot.

F. J. O. Corpuz, B. C. Y. Lafoteza, R. A. L. Broas and M. Ramos, "Design and implementation of a closed-loop static balance system for the YICAL Leg 2 biped," TENCON 2009 - 2009 IEEE Region 10 Conference, Singapore, 2009, pp. 1-6.

### Robot: YICAL Leg 2



Figure 2. The YICAL Leg II and its Kinematic Parameters [6]

### 16) Balance Recovery Analysis with Constraints of Feet ground for Biped Robot

[W. Yu, R. Zhuang and Z. Shao, "Balance recovery analysis with constraints of feet-ground for biped robot," 2017 IEEE International Conference on Mechatronics and Automation (ICMA), Takamatsu, 2017, pp. 1597-1601.]

A biped robot should be able to keep balance under unexpected disturbance, and can take up to four strategies, i.e. ankle, hip, step and reach & grasp strategies to recover balance. In this paper, the relationship between feet-ground constraints, namely the gravity constraints, the friction constraints and the Center of Pressure (CoP) constraints, and balance recovery strategy are analyzed. The satisfaction of these constraints-imposed bounds on the control torque is investigated. Finally, the friction coefficient and foot length/height ratio affect the joint torques to balance recovery, which can provide theoretical guidance for robot mechanism design.

**Robot:** two-link planar model

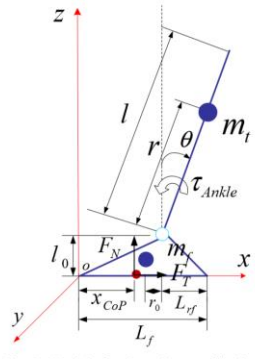


Fig. 2. Model of a planar humanoid robot

The dynamic equations are shown below:

$$\tau_{Ankle} = m_f g r \sin \theta - (I + m_f r^2) \ddot{\theta} \quad (1)$$

$$F_T = m_f r \ddot{\theta} \cos \theta - m_f r \dot{\theta}^2 \sin \theta \quad (2)$$

$$F_N = (m_f + m_t) g - m_f r \dot{\theta} \sin \theta - m_f r \dot{\theta}^2 \cos \theta \quad (3)$$

$$x_{CoP} = L_f - L_{rf} - \frac{l_0 F_T - \tau_{Ankle} + r_0 m_f g}{F_N} \quad (4)$$

**Fall Criteria:** There are four constraints between the feet and the ground during bipedal standing, namely, the gravity constraint, i.e., the feet do not lift from the ground; the friction constraint, i.e., the feet do not slide; the Center of Pressure (CoP) constraint, i.e., the center of pressure is within the contact surface between the feet and the ground, and the tip-over constraint, i.e., the biped robot does not rotate around the toe or the heel [12], [13]. The tip-over constraint can be characterized by the ZMP when both feet are on the same level ground

#### Threshold:

Three constraints can be written as:

$$F_N \geq 0 \quad (5)$$

$$|F_T| \leq \mu F_N \quad (6)$$

$$0 \leq x_{CoP} \leq L_f \quad (7)$$

#### Control Policy:

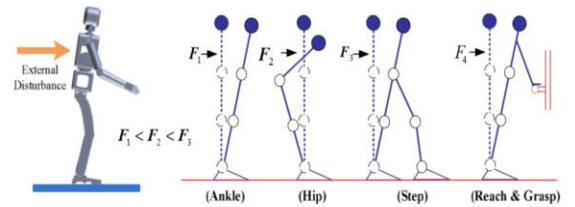


Fig. 1 The four basic balancing strategies in the presence of unknown external force

#### Friction Constraint and COP Constraint:

The control torque should be:

$$\max(\tau_{slip-anterior}, \tau_{cop-toe}) \leq \tau \leq \min(\tau_{slip-posterior}, \tau_{cop-heel}) \quad (16)$$

and simultaneously satisfy the following conditions:

$$\tau_{cop-heel} > \tau_{cop-toe} \quad (17)$$

$$\tau_{slip-posterior} > \tau_{slip-anterior} \quad (18)$$

$$\left\{ \begin{array}{l} \tau_{slip-posterior} = m_f g r \sin \theta \\ \quad + \frac{I + m_f r^2}{\Delta_2} [\mu(m_f + m_t)g - m_f r \dot{\theta}^2 (\sin \theta + \mu \cos \theta)] \end{array} \right. \quad (9)$$

$$\left\{ \begin{array}{l} \tau_{slip-anterior} = m_f g r \sin \theta \\ \quad + \frac{I + m_f r^2}{\Delta_3} [m_f r \dot{\theta}^2 (\mu \cos \theta - \sin \theta) - \mu(m_f + m_t)g] \end{array} \right. \quad (10)$$

And  $\Delta_2 = m_f r (\cos \theta - \mu \sin \theta)$ ,  $\Delta_3 = m_f r (\cos \theta + \mu \sin \theta)$

$$\left\{ \begin{array}{l} \tau_{cop-toe} = \frac{1}{\Delta_4} \{m_f r m_g r \sin \theta (L_{rf} \sin \theta - l_0 \cos \theta) \\ \quad + (I + m_f r^2) [m_f r \dot{\theta}^2 (L_{rf} \cos \theta + l_0 \sin \theta) - (0.5 L_f m_f + L_{rf} m_t) g]\} \end{array} \right. \quad (11)$$

$$\left\{ \begin{array}{l} \tau_{cop-heel} = \frac{1}{\Delta_5} \{m_f r m_g r \sin \theta (L_f \sin \theta - L_{rf} \cos \theta) \\ \quad + (I + m_f r^2) m_f r \dot{\theta}^2 [(L_f - L_{rf}) \cos \theta - l_0 \sin \theta] \\ \quad - (I + m_f r^2) [0.5 L_f m_f + (L_f - L_{rf}) m_t] g\} \end{array} \right. \quad (12)$$

$$\text{where } \Delta_4 = m_f r (L_{rf} \sin \theta - l_0 \cos \theta) - (I + m_f r^2) \quad ,$$

## 17) Falling Avoidance of Biped Robot using State Classification

[J. Kim, T. Choi and J. Lee, "Falling avoidance of biped robot using state classification," 2008 IEEE International Conference on Mechatronics and Automation, Takamatsu, 2008, pp. 72-76.]

The method uses a Support Vector machine (SVM) to classify the state. The input vector for the SVM are a magnitude of acceleration, a position of center of pressure (CoP) in x and z axis, and tilt angles of torso relative to x and z axis. The input vector is based on sensor data that is measured from accelerometer and force sensing resistor (FSR) sensor. Training of the classifier is done in off-line and the trained classifier is used to classify the state of the biped robot in on-line.

**Robot:** The biped robot considered in this paper has only lower body and consists of a left leg, a right leg and a waist. Each leg has 3 degrees of freedom as shown in Fig. 3. Two DOFs, one DOF and two DOFs are allocated for each hip joint, knee joint and ankle joints respectively.

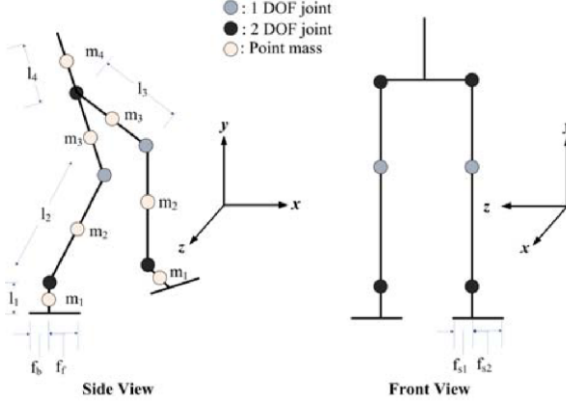


Fig. 3. The model of the biped robot

**Fall Criteria:** State classification method: The method classifies a falling state of biped robot based on data from

- 1)accelerometer
- 2) force sensing resistor (FSR)

Six features are selected to classify the state. The features are  
 1) magnitude of acceleration,  
 2)a position of Center of Pressure (CoP) in x and z axis, and  
 3)tilt angles of torso relative to x and z axis.

$$mag_{acc} = \sqrt{acc_x \times acc_x + acc_y \times acc_y + acc_z \times acc_z} \quad (1)$$

where  $acc_x$ ,  $acc_y$  and  $acc_z$  are acceleration of torso in x, y, z respectively.

The CoP is calculated by equation 2 and 3

$$x_{CoP} = \frac{\sum_{i=1}^n F_i x_i}{\sum_{i=1}^n F_i} \quad (2)$$

$$z_{CoP} = \frac{\sum_{i=1}^n F_i z_i}{\sum_{i=1}^n F_i} \quad (3)$$

where  $n$  is a total number of FSR sensor and  $F_i$  is a measured force at  $i$ th FSR. The features are scaled to from -1.0 to 1.0 when it is used as input of the classifier. Those feature is used for input vector of classifier and represented as equation 4

$$\mathbf{x}_t = (mag_{acc}, x_{CoP}, z_{CoP}, x_{tilt}, z_{tilt}) \quad (4)$$

### Threshold:

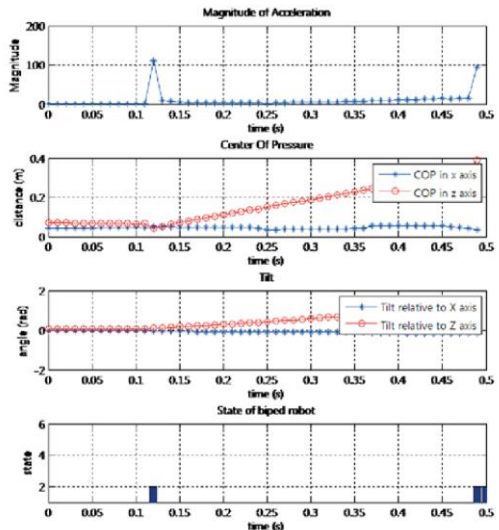


Fig. 4. State classification for left falling

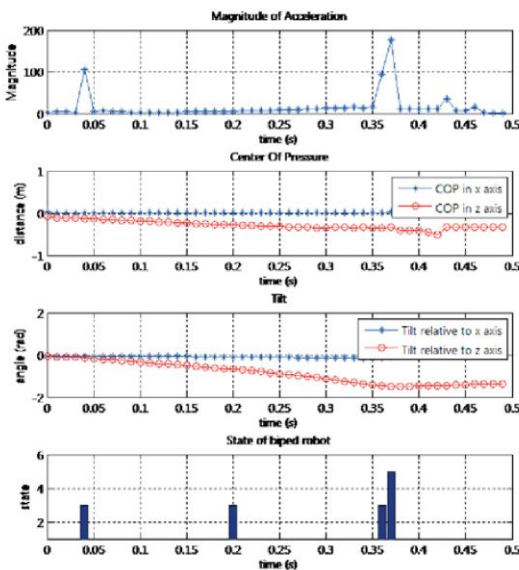


Fig. 5. State classification for right falling

**Control Policy:** the features and desired states are used to train a classifier with a Support Vector Machine (SVM). During a training phase, the biped robot collects example data for each class and trains the classifier on the data. After that, the classifier assigns any newly collected terrain data to one of the classes. The robot can now adapt its locomotion to the state, based on the classification result. For example, if the biped robot detects falling, it can step up its leg to prevent falling. The method is verified in a 3D dynamics simulator.

## 18) Effects of Joint Torque Constraints on Humanoid Robot Balance Recovery in the Presence of External Disturbance

[W. Yu, G. Bao and Z. Wang, "Effects of joint torque constraints on humanoid robot balance recovery in the presence of external disturbance," 2009 IEEE International Conference on Robotics and Biomimetics (ROBIO), Guilin, 2009, pp. 2362-2367.]

In this paper, the relationship between limited joint torque and balance recovery strategy is analyzed using Zero moment Point Manipulability Ellipsoid. Furthermore, during balance control, the constraints between the feet and the ground must be maintained. The satisfaction of these constraints, namely the gravity constraints, the friction constraints and the CoP constraints, imposed bounds on the control torque are investigated. Such control bounds have significant effects on designing balance recovery strategies and can be used to predict the type of falls.

**Robot:** 3 link model

**Fall criteria:** ZMP

**Threshold:** When ZMP is within the foot-support polygon, the humanoid robot is stability. After in the presence of external force, ZMP is reaching the edge of the foot-support

polygon resulting in the humanoid robot starting to tip over as shown in Fig. 2.

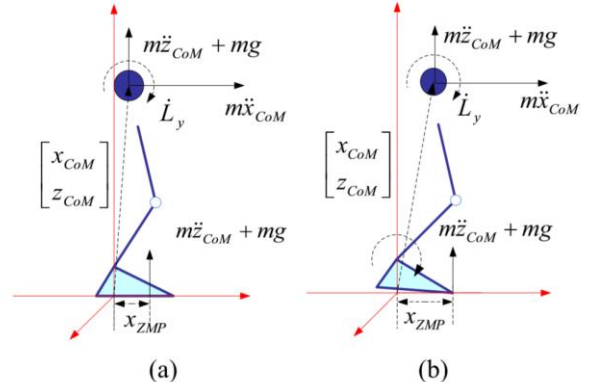


Fig. 2. (a) ZMP within the foot-support polygon (b) ZMP reaching the edge of the foot-support polygon resulting in the humanoid robot starting to tip over

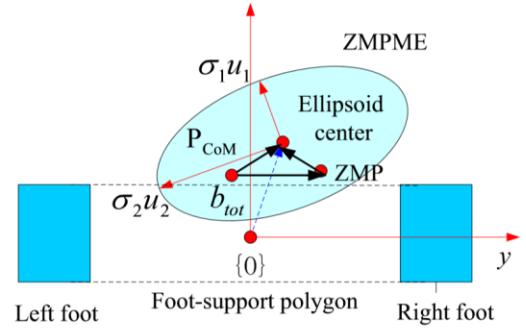


Fig. 3. The ZMPME and the relationship among the CoM, the ZMP, and the center of ellipsoid

By assuming that the change in the angular momentum at the CoM as well as the vertical CoM movement are negligible,  $b_{tot}$  becomes  $b_{tot} = p_{CoM} + z_{CoM} \dot{J}_{CoM} \dot{q} / g$ , which means the distance from the location of CoM to the center of the ZMPME is  $z_{CoM} \dot{J}_{CoM} \dot{q} / g$ . In a similar way, the distance from the location of CoM to ZMP is  $z_{CoM} \ddot{p}_{CoM} / g$ , and the distance from ZMP to the center of the ZMPME is  $z_{CoM} J_{CoM} \ddot{q} / g$ .

**Control policy:**

When the humanoid robot is subjected to a sudden external force, the humanoid robot will be instability because the ZMP leaves the foot-support polygon. In this case, if the ZMP ellipsoid overlaps the base of support, there exists a common area of the ZMP manipulability ellipsoid and the base of support, and the humanoid robot can regain balance by joint-torque control including ankle and hip strategies. If the ZMP ellipsoid does not overlap the base of support, the humanoid does not have adequate actuating torque to move ZMP inside the stability area and need step strategy to recovery balance.

### 19) A Universal Stability Criterion of the Foot Contact of Legged Robots - Adios ZMP

[H. Hirukawa et al., "A universal stability criterion of the foot contact of legged robots - adios ZMP," Proceedings 2006 IEEE International Conference on Robotics and Automation, 2006. ICRA 2006., Orlando, FL, 2006, pp. 1976-1983.]

The stability of the foot contact of a legged robot can be determined by checking the ZMP is inside the support polygon of the feet of the robot without solving the equations of motions when the robot is walking on a horizontal plane with sufficient friction. But a legged robot may walk on stairs or a rough terrain, and/or move using its hands as well as its feet. Besides, the friction between the robot and the environment may not be enough to prevent the robot from slipping. Therefore, the criteria of Sum of the gravity and the inertia wrench applied to the COG of the robot.

**Robot:** General biped

**Fall criteria:** Sum of the gravity and the inertia wrench applied to the COG of the robot

**Threshold:** If the sum of the gravity and the inertia wrench applied to the COG of the robot, which is proposed to be the stability criterion, is inside the polyhedral convex cone of the contact wrench between the feet of a robot and its environment.

It is proved that the determination is equivalent to check if the ZMP is inside the support polygon of the feet when the robot walks on a horizontal floor with sufficient friction.

### 20) Ankle and hip strategies for balance recovery of a biped subjected to an impact

[D. N. Nenchev and A. Nishio, "Experimental validation of ankle and hip strategies for balance recovery with a biped subjected to an impact," 2007 IEEE/RSJ International Conference on Intelligent Robots and Systems, San Diego, CA, 2007, pp. 4035-4040.]

we show how to implement two such reaction patterns, called ankle and hip strategy, using a small humanoid robot. Talk about Goswami

### Robot: 3 link model

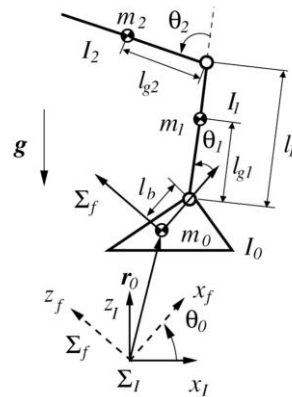


Fig. 1. Model of a planar biped in midair.

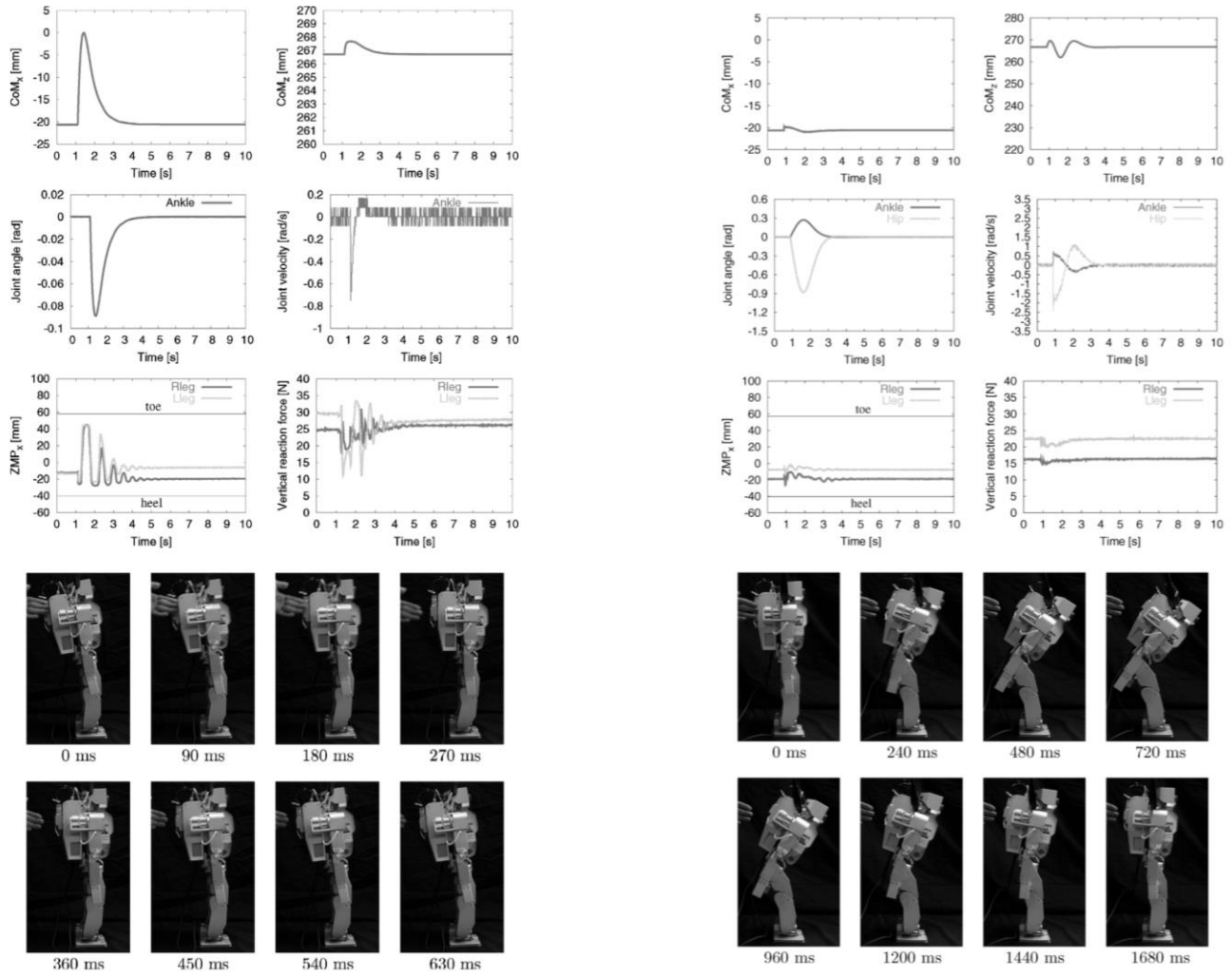
**Fall Criteria:** ZMP. The decision for invoking one of the reaction patterns is based on acceleration data measured during the impact.

**Threshold:** BOS

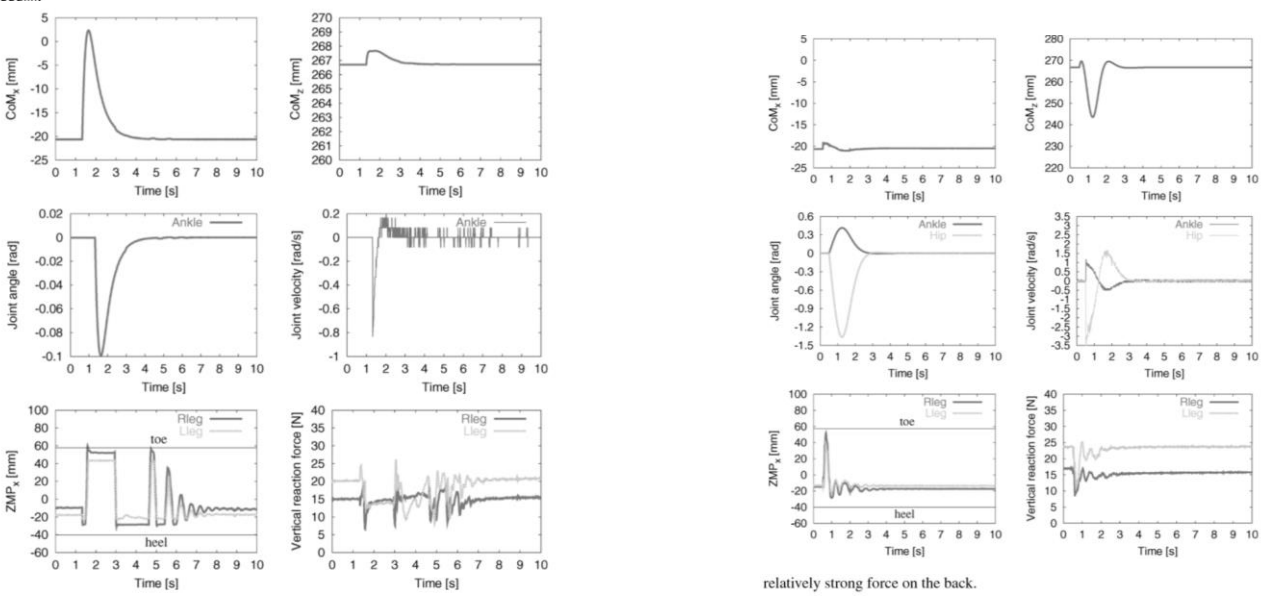
**Control Policy:**

The ankle strategy, for example, displaces the CoM slightly when the standing upright posture is perturbed. It was found out that this strategy is realized through ankle torque only. The hip strategy, on the other hand, minimizes the displacement of the CoM from the vertical by applying a torque in the hips mainly.

With a gentle push on the back, the human body reacts with the ankle strategy. With a stronger push, balance can be maintained by bending in the hips, i.e., with the hip strategy. When the acting force becomes even stronger, then to maintain balance, the BoS has to be changed, e.g., by making a step.



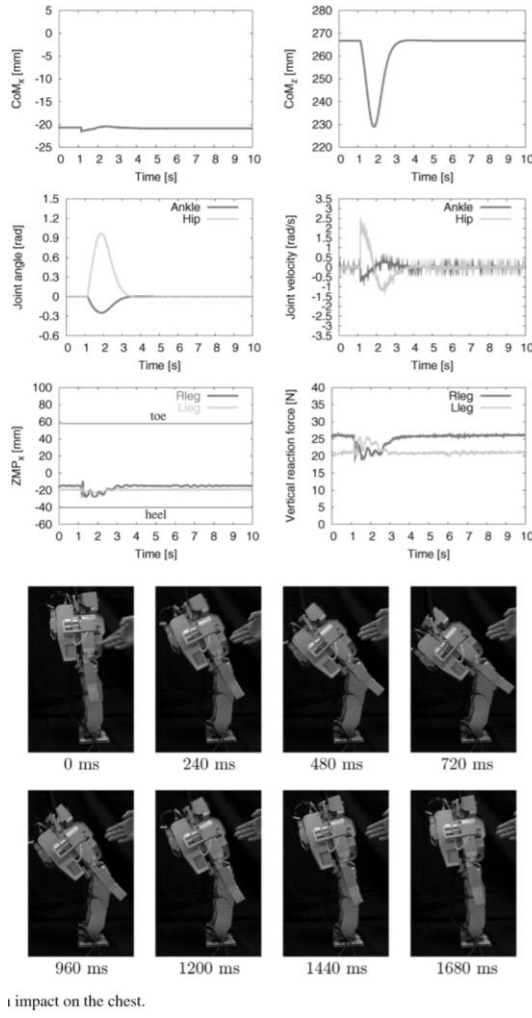
a relatively weak force on the back.



relatively strong force on the back.

not success.

## Fall Criteria and Balance Control of Legged Robots: Literature Review and Analysis

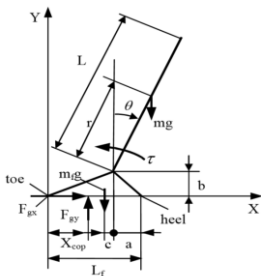


### 21) On the Effects of Constraints on Bipedal Balance Control during Standing

[C. Yang and Q. Wu, "On the Effects of Constraints on Bipedal Balance Control during Standing," 2007 American Control Conference, New York, NY, 2007, pp. 2842-2847.]

In this work, three sets of key parameters, namely the friction coefficient, the foot-link length, and the location of the mass center are varied to analyze their effects on balancing of biped.

**Robot:** 2 link model



### Fall Criteria:

#### Threshold:

$$\tau = mgr \sin \theta - (I + mr^2) \ddot{\theta} \quad (1a)$$

$$F_{gx} = mr\dot{\theta} \cos \theta - mr\dot{\theta}^2 \sin \theta \quad (1b)$$

$$F_{gy} = (m_f + m)g - mr\ddot{\theta} \sin \theta - mr\dot{\theta}^2 \cos \theta \quad (1c)$$

The gravity constraint requires that the vertical ground force ( $gy$  F) be upward. The friction constraint requires that the horizontal ground force ( $gx$  F) be lower than the maximum static friction. The COP constraint requires that the pressure center (COP x ) be between the toe and the heel indicating that the rotation about the toe and the heel does not occur. The three constraints are written as:

$$F_{gy} \geq 0$$

$$|F_{gx}| \leq \mu F_{gy}$$

$$0 \leq x_{cop} \leq L_f$$

### 22) Rate of change of angular momentum and balance maintenance of biped robots

[A. Goswami and V. Kallem, "Rate of change of angular momentum and balance maintenance of biped robots," IEEE International Conference on Robotics and Automation, 2004. Proceedings. ICRA '04. 2004, New Orleans, LA, USA, 2004, pp. 3785-3790 Vol.4.]

Our research focuses on HG, the rate of change of centroidal angular momentum of a robot, as the physical quantity containing its stability information. We propose three control strategies using HG that can be used for stability recapture of biped robots.

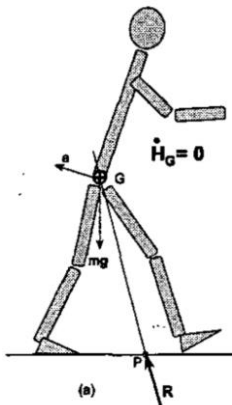
#### Robot:

**Fall Criteria:** the resultant external moment on a system, computed at its CoM, is equal to the rate of change of its centroidal angular momentum  $H_C$

**Threshold:** For free walk on horizontal ground, a derived criterion refers to a point on the foot/ground surface of a robot where the total ground reaction force would have to act such that :

$$H_G = \mathbf{0}$$

That is a biped robot is considered rotationally stable if the external forces and moments sum up to a zero centroidal moment.

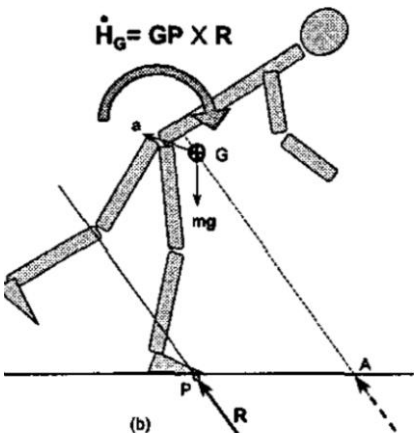
**Control Policy:**

an unstable biped ( $\dot{H}_G \neq 0$ ) could be stabilized by shifting the GRF Line of action appropriately such that it passes through the CoM.

This also causes the GRF Line of action to penetrate the ground at a different point, and this point might not lie within the convex hull of the foot support area. If the GRF were to act through this shifted point (point A in Fig. Ib), while maintaining its original direction,  $H_G$  would reduce to zero. We name point A the ZRAM point zero gate of change of Angular Momentum).

It can be achieved using following strategy:

- 1) Enlarge support polygon such that it encompasses the ZRAM point A.
- 2) Move G with respect to P such that R passes through G in its new location  $G'$ .

**23) Control Strategy Research for a Biped Walking Robot with Flexible Ankle Joints**

[X. Zang, Z. Lin, Y. Liu, X. Sun and J. Zhao, "Control Strategy Research for a Biped Walking Robot with Flexible Ankle Joints," 2017 First IEEE International Conference on Robotic Computing (IRC), Taichung, 2017, pp. 93-96.]

X. Zang, Z. Lin, Y. Liu, X. Sun and J. Zhao, "Control Strategy Research for a Biped Walking Robot with Flexible Ankle Joints," 2017 First IEEE International Conference on Robotic Computing (IRC), Taichung, 2017, pp. 93-96.

**Robot:** 7DOF

**Fall Criteria:** Limit Cycle

**Threshold:**

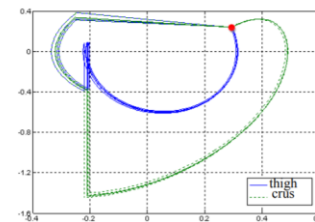


Figure 4. The swing leg limit cycle.

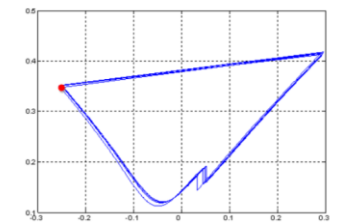


Figure 5. The supporting leg limit cycle.

**24) Push Recovery Methods Based on Admittance Control Strategies for a NAO-H25 Humanoid**

[F. S. Mousavi, M. Tale Masouleh, A. Kalhor and P. Ghassemi, "Push Recovery Methods Based on Admittance Control Strategies for a NAO-H25 Humanoid," 2018 6th RSI International Conference on Robotics and Mechatronics (IcRoM), Tehran, Iran, 2018, pp. 451-457.]

The first part indicates the simulation results of different strategies retrieved from human behaviors, namely: Ankle, Hip, and Hip ankle strategies. These methods are separately assessed and their efficiencies are discussed.

**Robot:** NAO H25

**Fall Criteria:** ZMP

**Threshold:** SP

**Control Policy:** The main objective of this paper was about push recovery of a NAO H-25 robot regarding three strategies inspired from human behavior: (1) Ankle strategy (2) Hip strategy (3) Hip ankle strategy. These methods were evaluated by simulation by NAO H-25 robot's simulator.

## Fall Criteria and Balance Control of Legged Robots: Literature Review and Analysis

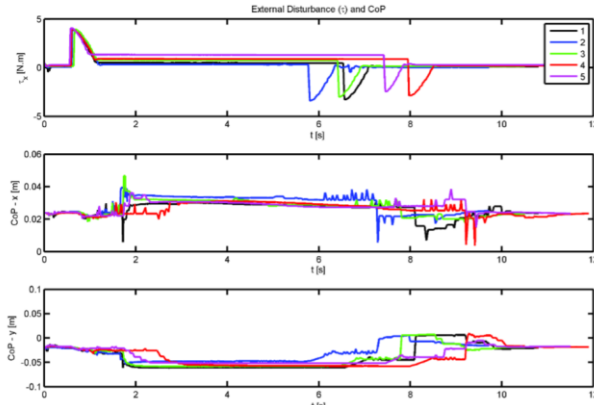


Figure 8: Results of robot's output for admittance controller: predicted external disturbance and CoP (simulation).

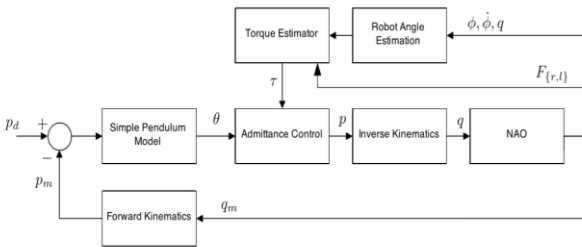


Figure 6: The block diagram for the proposed admittance controller.

NAO—no disturbance sensor- Kalman filter for the purpose of disturbance prediction

Afterward, admittance control is considered as a means of push recovery against disturbances based on the location and force information.

One foot in contact: ZMP criteria

Higher disturbance: Modeled by a second-order mass-spring-damper system, which absorbs the external disturbance's energy. (ZMP doesn't work when something else than legs is in contact with the environment)

### 25) How to Keep from Falling Forward: Elementary Swing Leg Action for Passive Dynamic Walkers

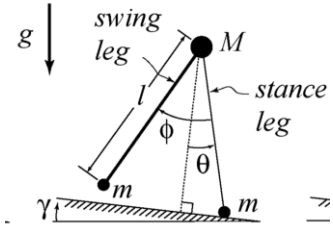
[M. Wisse, A. L. Schwab, R. Q. van der Linde and F. C. T. van der Helm, "How to keep from falling forward: elementary swing leg action for passive dynamic walkers," in IEEE Transactions on Robotics, vol. 21, no. 3, pp. 393-401, June 2005.]

They show that it is impossible for any form of swing leg control to solve backward falling. For the problem of forward falling, they devise a simple but very effective rule for swing leg action:

**"You will never fall forward if you put your swing leg fast enough in front of your stance leg. In order to prevent falling backward the next step, the swingleg shouldn't be too far in front."**

**Robot:** Prototype Mike: 2-D passive dynamic walking robot with pneumatic McKibben muscles at the hip.

**Fall Criteria:** the initial conditions of the next step are only



a function of  $\theta$  and  $\dot{\theta}$ .

**Threshold:** The entire collection of initial conditions leading to walking is what is called the basin of attraction. In Fig.4 the basin of attraction is represented by the very thin area A, otherwise the walker falls forward or backward. [http://www.scholarpedia.org/article/Basin\\_of\\_attraction](http://www.scholarpedia.org/article/Basin_of_attraction)

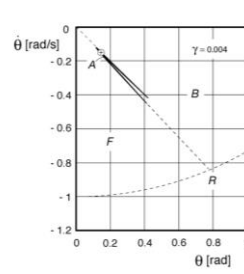
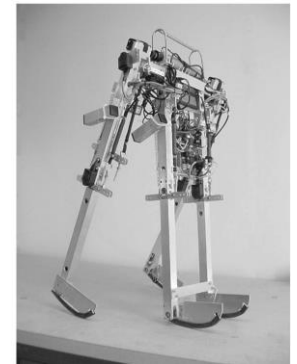


Fig. 4. Poincaré section for the simplest walker with initial stance leg angle  $\theta$  and velocity  $\dot{\theta}$  together with failure modes: falling Forward, falling Backward and the basin of attraction of the cyclic walking motion  $(\theta, \dot{\theta}) = (0.1534, -0.1561)$  (indicated with “+”) at a slope of  $\gamma = 0.004$  rad. Reprinted from [20].



### Control Policy: Stepping

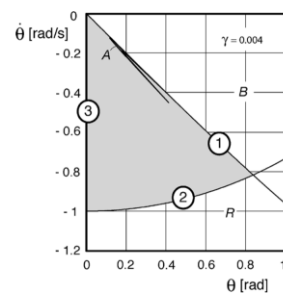


Fig. 5. Maximally obtainable basin of attraction (gray area, bounded by Lines 1, 2 and 3, see text) and uncontrolled basin of attraction (thin area A) of the simplest walking model. The entire problem of falling forward can be solved with swing leg control, while the problem of falling backward (area B) remains existent and would need something else than swing leg control.

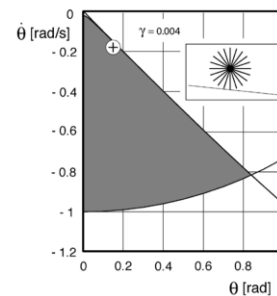


Fig. 6. Basin of attraction of the rimless wheel (model: see inset) with an interspoke angle of 0.3 rad. The initial conditions to the right of the dashed line can only be realized by starting at the top edge of a table. The “+” indicates the fixed point of this model at a slope of  $\gamma = 0.004$  rad.

## 26) A Robust Walking Controller Based on Online Optimization of Ankle, Hip, and Stepping Strategies

[H. Jeong, I. Lee, J. Oh, K. K. Lee and J. Oh, "A Robust Walking Controller Based on Online Optimization of Ankle, Hip, and Stepping Strategies," in IEEE Transactions on Robotics, vol. 35, no. 6, pp. 1367-1386, Dec. 2019.]

propose a biped walking controller that optimized three push recovery strategies: the ankle, hip, and stepping strategies.

**Robot:** GAZELLE – 13 DOF biped

**Fall Criteria:** DCM Offset (DCM- divergent component of motion) (Simulation on Linear inverted pendulum with flywheel model to verify the effectiveness of the algorithm.)  
DCM:

$$\xi = \mathbf{x} + \frac{\dot{\mathbf{x}}}{\omega}$$

Where X=CoM

DCM Offset:

The DCM offset is the difference between the point at which the DCM arrives and the foot landing position at the end of current step.

$$\mathbf{b} = \xi_T - \mathbf{u}_T.$$

**Threshold:**

If the robot has bigger DCM offset than the value of (15), it will fall over.

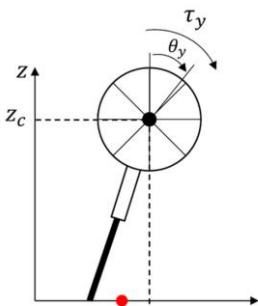
$$b_{x,\max} = \frac{L_{\max}}{e^{\omega T_{\min}} - 1}.$$

maximum foot stride (Lmax) and minimum step time (Tmin)

**Control Policy:**

Ankle Strategy: controlling the ZMP or the Center of Pressure (CoP),which is controllable by acceleration of the CoM or ankle torque.

Stepping Strategy: generating online walking patterns using model predictive control (MPC). The MPC approach is able to change the step position by setting it as an optimization variable and by restricting the ZMP inside the sole. Also, stabilize the gait more efficiently by modifying the step time as well as the step position.



## 27) A Push-Recovery Method for Walking Biped Robot Based on 3-D Flywheel Model

[R. C. Luo and C. Huang, "A push-recovery method for walking biped robot based on 3-D flywheel model," IECON 2015 - 41st Annual Conference of the IEEE Industrial Electronics Society, Yokohama, 2015, pp. 002685-002690.]

**Robot:** iCeiRA – 2 leg + trunk

**Fall Criteria:** ZMP (Simulated using Linear inverted pendulum plus flywheel model in sagittal plane- The LIPFM takes the effect of rotary inertia and reaction mass into account.)

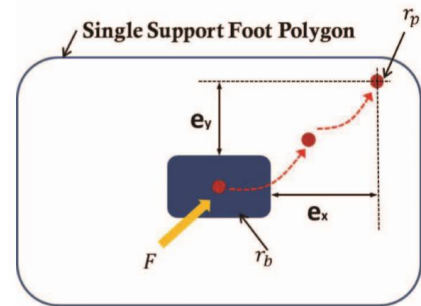


Fig. 4. The offset of ZMP in planar view by perturbation and safe region.

**Threshold:** Support Polygon (The acceleration of CoG is an indicator of external disturbance- FT sensor.)

**Control Policy:** External disturbance is detected when there is a spike in FT sensor value of CoG. Stepping and Trunk rotate strategies are used. ZMP comes back within SP. Then Preview control for normal walking. <https://ieeexplore.ieee.org.proxy.library.nyu.edu/stamp/stamp.jsp?tp=&arnumber=1241826>

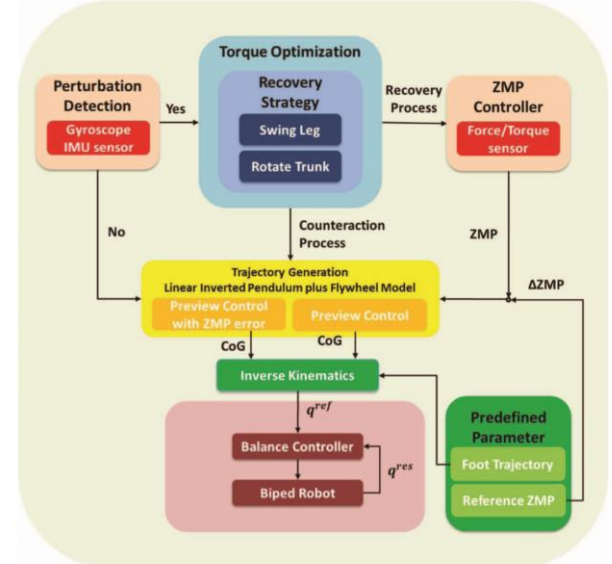


Fig. 2. Overall control architecture.

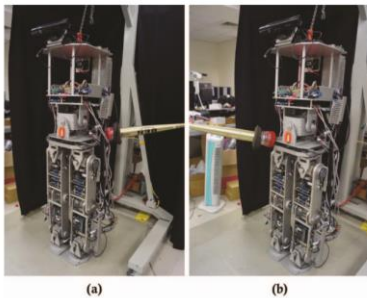


Fig. 8. Relation between the biped robot and pushing force. (a) The force is from left rear of robot in the second step. (b) The force is from right front of robot in the fourth step.

## 28) Stepping Stabilization Using a Combination of DCM Tracking and Step Adjustment

[M. Khadiv, S. Kleff, A. Herzog, S. A. A. Moosavian, S. Schaal and L. Righetti, "Stepping stabilization using a combination of DCM tracking and step adjustment," 2016 4th International Conference on Robotics and Mechatronics (ICROM), Tehran, 2016, pp. 130-135.]

**Robot:** Linear Inverted Pendulum Model (LIPM)



### Fall Criteria:

DCM - Divergent Component of Motion

$$(\xi = x + \dot{x}/\omega_0)$$

$$\omega_0 = \sqrt{g/z_0}$$

x is a 2-D vector containing CoM horizontal components  
z0 is the CoM height

DCM Trajectory:

$$\xi(t) = (\xi_0 - u)e^{\omega_0 t} + u$$

$\xi_0$  and u are the DCM and CoP at the beginning of a step

t is step period

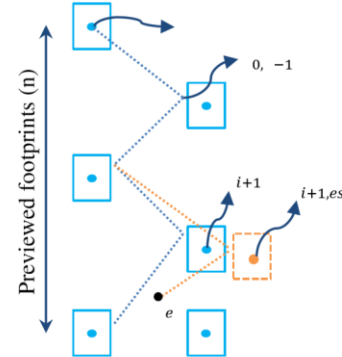
### Threshold:

DCM (its projection on the ground) coincident with the footprint at the end of a previewed number of steps.

### Control Policy:

Stepping:

- a) The foot trajectory is modified to compensate for the DCM tracking error.



$$u_{i+1,es} = \frac{\xi_{0,i+2} - \xi_{0,i+1,es} e^{\omega_0 T}}{1 - e^{\omega_0 T}} , \quad 0 \leq t \leq T$$

## 29) A Robust Biped Locomotion Based on Linear-Quadratic-Gaussian Controller and Divergent Component of Motion

[M. Kasaei, N. Lau and A. Pereira, "A Robust Biped Locomotion Based on Linear-Quadratic-Gaussian Controller and Divergent Component of Motion," 2019 IEEE/RSJ International Conference on Intelligent Robots and Systems (IROS), Macau, China, 2019, pp. 1429-1434.]

**Robot:** Linear Inverted Pendulum Model (LIPM)

$$\ddot{x} = \omega^2(x - p_x)$$

$$\omega = \sqrt{\frac{g+z}{z}}$$

x is a 2-D vector containing CoM horizontal components

z0 is the CoM height

Px is position of ZMP

**Fall Criteria:** DCM - Divergent Component of Motion  
The unstable part of COM dynamics is called DCM and conceptually it is the point that robot should step to come to rest over the support foot.

$$\zeta = x + \frac{\dot{x}}{\omega}$$

### Threshold:

DCM (its projection on the ground) coincident with the footprint at the end of a previewed number of steps.

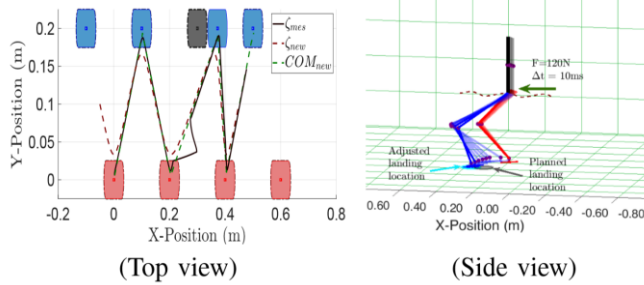
### Control Policy:

### Online Foot Step Adjustment

the robot should change the landing location of the swing leg to regain its stability. According to the observability of DCM at each control cycle, the position of DCM at the end of the step can be predicted in advance:

$$p_{x+1} = p_x + (\zeta_t - p_x)e^{w(T-t)}$$

$p_{x+1}$  is the next footstep position,  $t, T, \zeta_t$  represent the time, step duration and measured DCM respectively



### 30) A Model-Based Biped Walking Controller Based on Divergent Component of Motion

[M. M. Kasaei, N. Lau and A. Pereira, "A Model-Based Biped Walking Controller Based on Divergent Component of Motion," 2019 IEEE International Conference on Autonomous Robot Systems and Competitions (ICARSC), Porto, Portugal, 2019, pp. 1-6.]

**Robot:** Linear Inverted Pendulum Plus Flywheel Model (ELIPPFM)

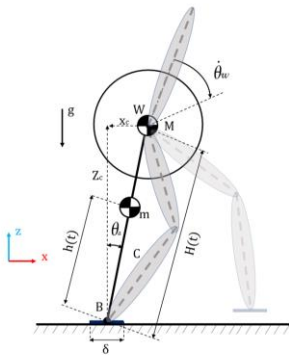


Fig. 1. Dynamics model of a humanoid robot in the single support phase with a flywheel body and considering mass of stance leg. In this model, swing leg is considered to be massless. Two actuators are used which are located at the flywheel center (equal to COM of robot) and at the ankle.

**Fall Criteria:** DCM - Divergent Component of Motion

$$\zeta_x = x_c + \frac{\dot{x}_c}{\omega}$$

$$\omega^2 = \frac{g+z_c}{z_c}$$

$x_c$  is CoM component in x direction

$z_c$  is CoM component in z direction

$z_c$  is the CoM height

### Threshold:

$$\Delta \dot{\zeta} = |\dot{\zeta}_r - \dot{\zeta}_x| > thr_2.$$

where  $\zeta_r, \zeta_x$  are the reference and actual DCM position. It should be noted that  $thr_1, thr_2$  are defined by trial and error.

### Control Policy:

Changing Swing leg landing position.

$$P_{sw_{new}} = P_{sw} + (\zeta_{xT} - \zeta_{rT})$$

where  $P_{sw_{new}}$  and  $P_{sw}$  represent the new and the planned swing leg positions,  $\zeta_{xT}, \zeta_{rT}$  are the reference and actual DCM positions at the end of step.

### 31) Balancing and Walking Using Full Dynamics LQR Control with Contact Constraints

[S. Mason, N. Rotella, S. Schaal and L. Righetti, "Balancing and walking using full dynamics LQR control with contact constraints," 2016 IEEE-RAS 16th International Conference on Humanoid Robots (Humanoids), Cancun, 2016, pp. 63-68.]

**Robot:** 2 DOF biped

**Fall Criteria:**

**Threshold:**

**Control Policy:**

### 32) Differentially Flat Design of Bipeds Ensuring Limit-Cycles

[V. Sangwan and S. K. Agrawal, "Differentially Flat Design of Bipeds Ensuring Limit Cycles," in IEEE/ASME Transactions on Mechatronics, vol. 14, no. 6, pp. 647-657, Dec. 2009.]

**Robot:** 2 DOF biped

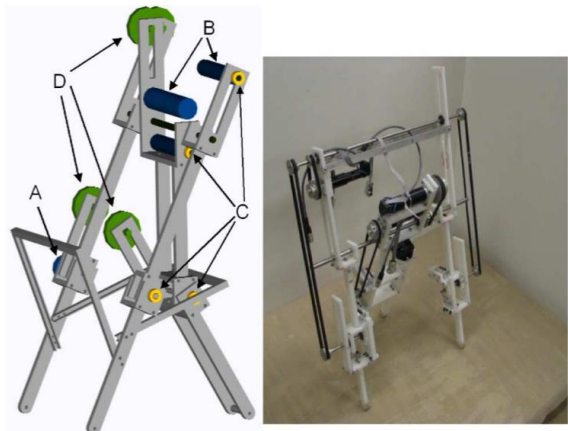


Fig. 9. 3-DOF planar biped robot. It has a shank and a thigh in each leg. The knee joint has a stopper to prevent hyperextension and there are latches (A) that lock the knee joint after the knee impact. Maxon motors (B) are placed at the hip and they drive the corresponding axis via a pulley (C) and belt arrangement. Counterweights (D) are used to place the COM at the respective joints.

**Fall Criteria:** Limit Cycle**Threshold:**

$$\begin{aligned} T &\leq T_{max}, & |\ddot{y}| &\leq 1, \\ -\frac{pi}{4} < q_1^- &< 0, & \dot{q}_1 &< 0, \\ N > 0, & & h > 0, \\ -0.08 < q_{m1} &< 0.08. & & \end{aligned}$$

The first constraint keeps the gait period in bounded. The second constraint is necessary for the diffeomorphism to exist. The third constraint ensures a reasonable initial state of the biped. The fourth constraint makes sure that the biped always moves forward. The fifth and sixth inequalities constrains the ground normal reaction  $N$  and heel height to be positive, respectively. The last constraint makes sure that the foot scuff happens in a nearly vertical configuration.

**Control Policy:** Change foot contact location.

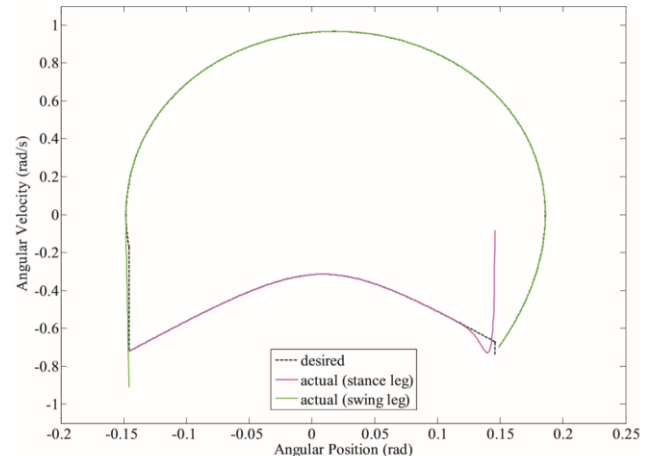
**Threshold:**

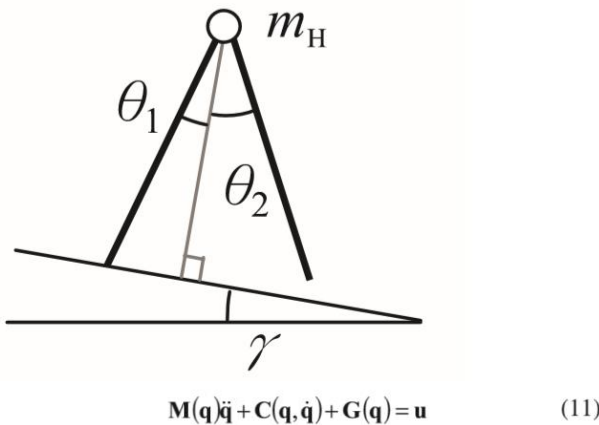
Fig. 3(a) Trajectory of the stance leg and the swing leg in the phase plane

**Control Policy:** Backstepping control

**33) Balancing and Walking Using Full Dynamics LQR Control With Contact Constraints**

[S. Mason, N. Rotella, S. Schaal and L. Righetti, "Balancing and walking using full dynamics LQR control with contact constraints," 2016 IEEE-RAS 16th International Conference on Humanoid Robots (Humanoids), Cancun, 2016, pp. 63-68.]

**Robot:** classic planar compass biped robot



$$\text{where } M(\mathbf{q}) = \begin{bmatrix} I + ma^2 + m_H l^2 + ml^2 & -mlb \cos(\theta_1 - \theta_2) \\ -mlb \cos(\theta_1 - \theta_2) & I + mb^2 \end{bmatrix},$$

$$C(\mathbf{q}, \dot{\mathbf{q}}) = \begin{bmatrix} -mlb \dot{\theta}_1 \dot{\theta}_2 \sin(\theta_1 - \theta_2) \\ mlb \dot{\theta}_1 \dot{\theta}_2 \sin(\theta_1 - \theta_2) \end{bmatrix},$$

$$G(\mathbf{q}) = \begin{bmatrix} -(mga + m_H gl + mgl) \sin(\theta_1 - \gamma) \\ mg b \sin(\theta_2 - \gamma) \end{bmatrix}, \text{ and } \mathbf{u} = \begin{bmatrix} \tau_1 + \tau_2 \\ -\tau_2 \end{bmatrix}.$$

**Fall Criteria:** Limit cycle in the phase plane

**34) Global stability analysis for plane limit cycle walking models with feet and actuation**

[Y. Jeon, Y. Park and Y. Park, "Global stability analysis for plane limit cycle walking models with feet and actuation," Proceedings of SICE Annual Conference 2010, Taipei, 2010, pp. 1812-1814.]

**Robot:** Planer compass models

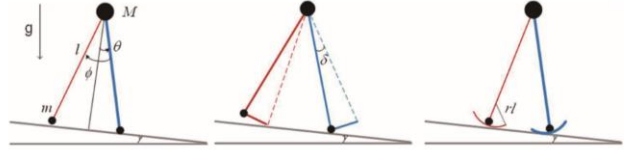


Figure 1. The simplest walker and modified walkers. In the middle, the model has flat feet. Curved feet model is on the right side. Bold line represents stance leg and another is swing leg.

**Fall Criteria:** Limit Cycle

**Threshold:** Basin of attraction

$[\delta]$  (a foot length) and  $r$  (radius of a foot),  $\gamma$  is a slope]

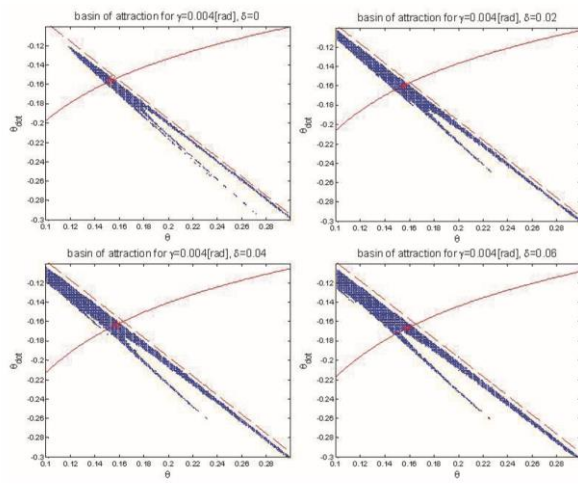


Figure 3. Basin of attraction of flat feet model. Solid line represents energy balance and dashed line represents falling boundary. the fixed point is marked with an asterisk and must be located on energy balance line.

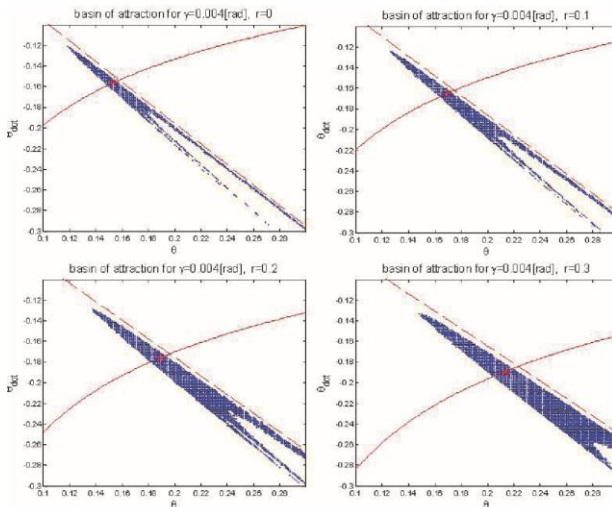


Figure 4. Basin of attraction of curved feet model. Solid line represents energy balance and dashed line represents falling boundary. the fixed point is marked with an asterisk.

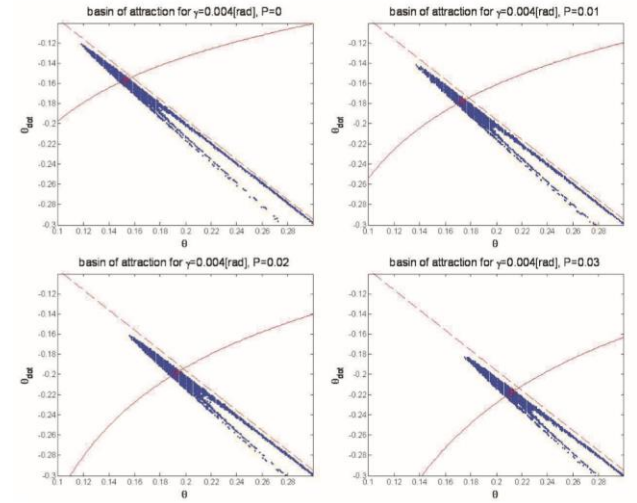


Figure 5. Basin of attraction of the model with toe-off. Solid line represents energy balance and dashed line represents falling boundary. the fixed point is marked with an asterisk.

**Control Policy:** Stepping, Toe-off impulse, Change In design

The falling boundary does not change, but the energy balance line changing as increasing the toe-off impulse. So, the fixed point is changed. However, The basin of attraction does not increase as changing the toe-off impulse.

### 35) Limit Cycle Based Walk of a Powered 7DOF 3D Biped with Flat Feet

[Y. Harada, J. Takahashi, D. Nenchev and D. Sato, "Limit cycle based walk of a powered 7DOF 3D biped with flat feet," 2010 IEEE/RSJ International Conference on Intelligent Robots and Systems, Taipei, 2010, pp. 3623-3628.]

#### Robot: 7DOF 3D Biped with Flat Feet

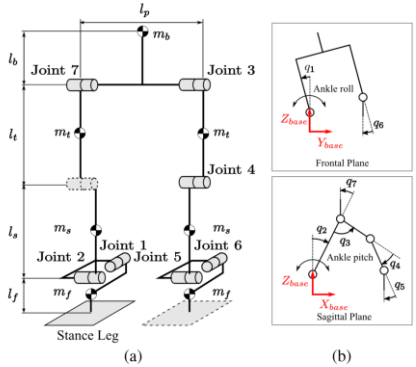


Fig. 1. 7DOF 3D biped model: (a) kinematic structure, (b) generalized coordinates of the model.

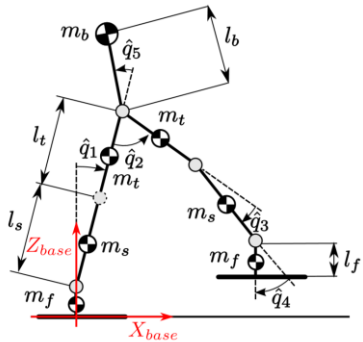


Fig. 2. Virtual 2D model.

#### Fall Criteria: Limit Cycle

#### Threshold:

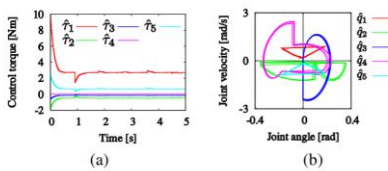


Fig. 5. Limit cycle based walking with the virtual 2D model (perfect dynamic model) using energy feedback control. Motion starts from the neighborhood of the stable equilibrium point: (a) control torque vs. time, (b) phase portrait.

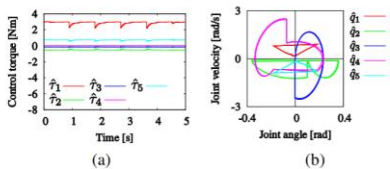


Fig. 6. Limit cycle based walking with the virtual 2D model (imperfect dynamic model) using energy feedback control. Motion starts at the stable equilibrium point: (a) control torque vs. time, (b) phase portrait.

#### Control Policy: Stepping

### 36) Stability Regions for Standing Balance of Biped Humanoid Robots

[J. H. Kim, J. Lee and Y. Oh, "Stability regions for standing balance of biped humanoid robots," 2017 IEEE International Conference on Robotics and Automation (ICRA), Singapore, 2017, pp. 4735-4740.]

#### Robot: LIPM linear inverted pendulum model

**Fall Criteria:** CoM position and velocity initial condition and ZMP

#### Threshold:

The position and velocity of the CoM tend to zero for its arbitrary bounded initial value when there is no external force disturbance.

The ZMP is always located inside the supporting region S.

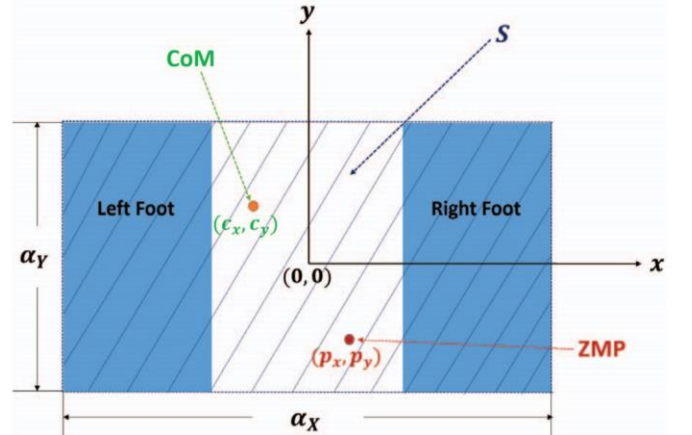
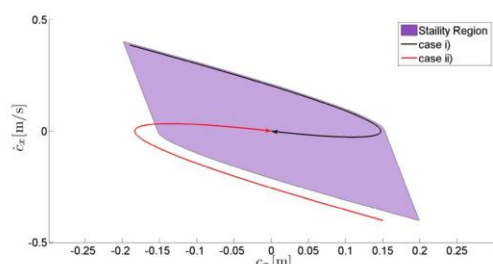


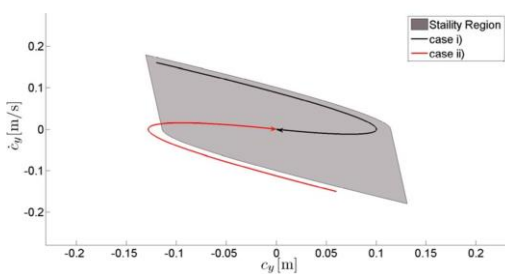
Fig. 2. Coordinates of  $x$ - $y$  plane and supporting region  $S$ .

These conditions are also mathematically represented by

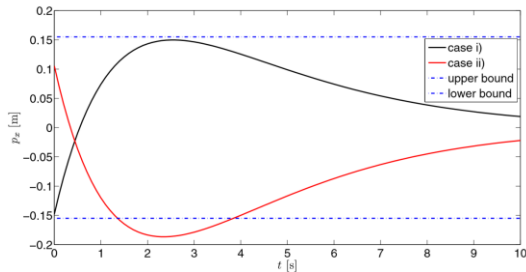
- (i)\*  $\dot{x}(t) \rightarrow 0$  ( $t \rightarrow \infty$ ) for an arbitrary  $x(0) \in \mathbb{R}^2$  such as  $|x(0)|_\infty < \infty$  when  $w(t) \equiv 0$  ( $\forall t \geq 0$ ).
- (ii)\*  $u(t) \in S$  ( $\forall t \geq 0$ ).



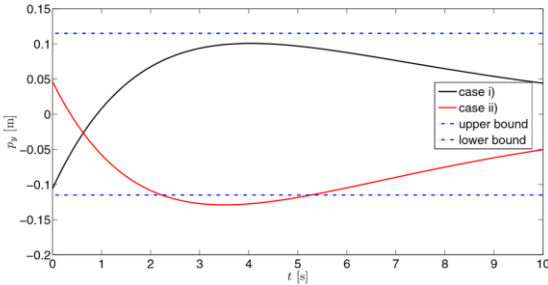
(a) Stability region for initial values of  $(c_x, \dot{c}_x)$ . i) The CoM trajectory  $(c_x, \dot{c}_x)$  always stays inside the stability region. ii) The CoM trajectory  $(c_x, \dot{c}_x)$  starts outside the stability region.



(a) Stability region for initial values of  $(c_y, \dot{c}_y)$ . i) The CoM trajectory  $(c_y, \dot{c}_y)$  always stays inside the stability region. ii) The CoM trajectory  $(c_y, \dot{c}_y)$  starts outside the stability region.



(b) ZMP trajectories for two cases. i)  $p_z$  with the initial value of  $(c_x, \dot{c}_x)$  inside the stability region. ii):  $p_z$  with the initial value of  $(c_x, \dot{c}_x)$  outside the stability region.



(b) ZMP trajectories for two cases. i)  $p_y$  with the initial value of  $(c_y, \dot{c}_y)$  inside the stability region. ii)  $p_y$  with the initial value of  $(c_y, \dot{c}_y)$  outside the stability region.

These observations clearly demonstrate the effectiveness and validity of the computation method discussed in Theorem 1 that corresponds to the stability region with respect to the initial values of the CoM position and velocity.

### 37) Study on Walking Stabilities of a Biped Robot in Considering the Distribution of Ground Reacting Forces Robot:

[X. Ke, Z. Gong and J. Wu, "Study on Walking Stabilities of a Biped Robot in Considering the Distribution of Ground Reacting Forces," 2006 International Conference on Mechatronics and Automation, Luoyang, Henan, 2006, pp. 1636-1641.]

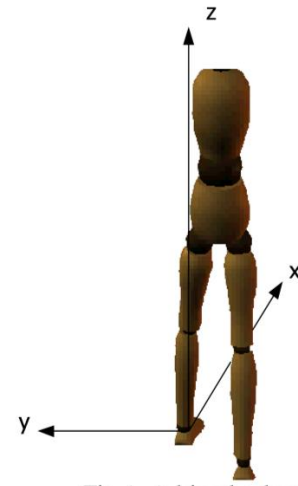
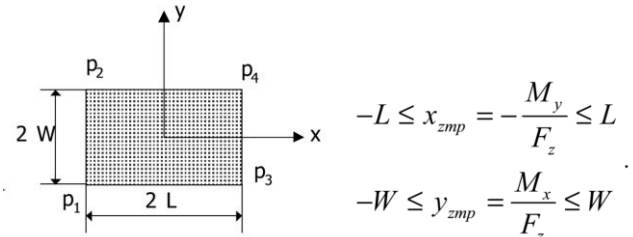


Fig.1. A biped robot

**Fall Criteria: ZMP**

**Threshold: support Polygon**



$$\begin{aligned} -L \leq x_{zmp} = -\frac{M_y}{F_z} \leq L \\ -W \leq y_{zmp} = \frac{M_x}{F_z} \leq W \end{aligned}$$

$$\begin{aligned} x_{\max} &= \left( \left| \frac{F_x}{F_z^+} - \frac{3M_x M_z}{F_z^2(L^2 + W^2) - 3(M_x^2 + M_y^2)} \right| \right. \\ &\quad \left. + \frac{3F_z |M_z|}{F_z^2(L^2 + W^2) - 3(M_x^2 + M_y^2)} W \right)^2 \\ y_{\max} &= \left( \left| \frac{F_y}{F_z^+} - \frac{3M_y M_z}{F_z^2(L^2 + W^2) - 3(M_x^2 + M_y^2)} \right| \right. \\ &\quad \left. + \frac{3F_z |M_z|}{F_z^2(L^2 + W^2) - 3(M_x^2 + M_y^2)} L \right)^2 \end{aligned} \quad (35)$$

then the final result is obtained:

$$\sqrt{x_{\max} + y_{\max}} \leq \mu_{\max}. \quad (36)$$

That is the necessary and sufficient condition for a biped robot having no slippage happened in the walking.

### 38) Energy-Efficient Gait Planning and Control for Biped Robots Utilizing the Allowable ZMP Region

[H. Shin and B. K. Kim, "Energy-Efficient Gait Planning and Control for Biped Robots Utilizing Vertical Body Motion and Allowable ZMP Region," in IEEE Transactions on Industrial Electronics, vol. 62, no. 4, pp. 2277-2286, April 2015.]

**Robot:** DARwIn-OP - 12 motorized joints – LIPM

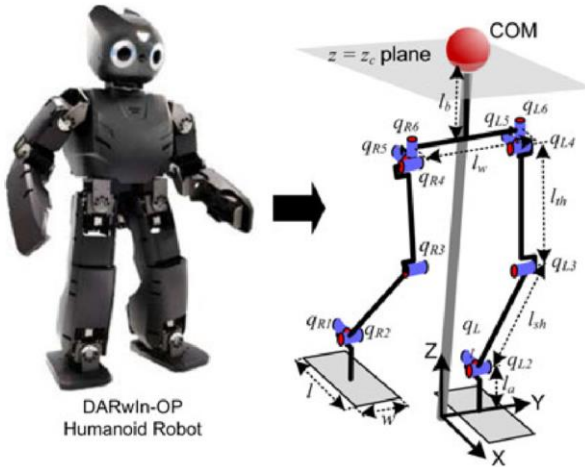


Fig. 1. Three-dimensional-biped robot model for the DARwIn-OP humanoid robot.

#### Fall Criteria: ZMP

**Threshold:** AZR- allowable ZMP region

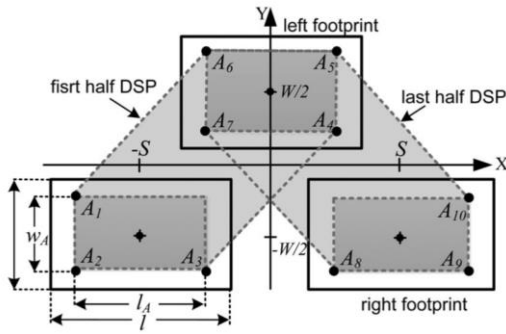


Fig. 2. Allowable ZMP Region. Interior of the dotted line is the AZR and the outer region of the AZR defines the stability margin naturally.

$$\begin{bmatrix} p(t) \\ q(t) \end{bmatrix} = \begin{bmatrix} x(t) \\ y(t) \end{bmatrix} - \frac{1}{\omega^2} \begin{bmatrix} \ddot{x}(t) \\ \ddot{y}(t) \end{bmatrix}, \quad \omega = \sqrt{g/z_C}.$$

ZMP Pzmp = [p, q, 0]

COM Pcom =[x,y,z]

#### Control Policy:

1. Changing step length and duration
2. Changing swing foot trajectory

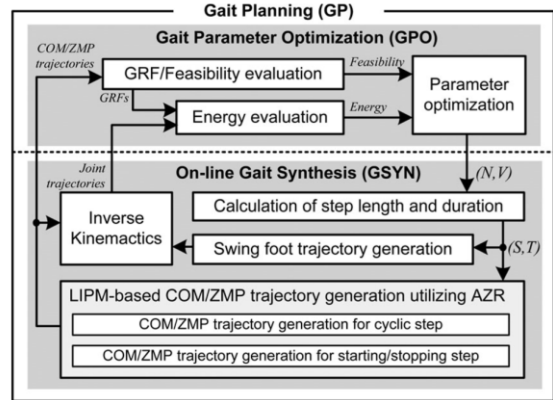
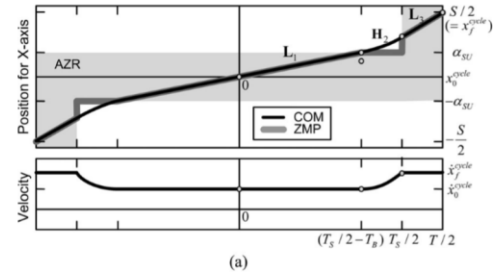
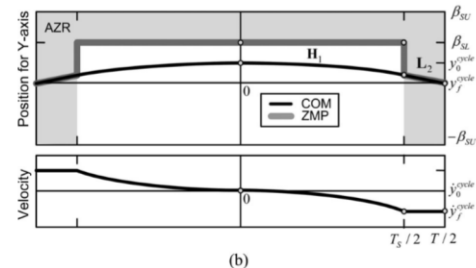


Fig. 3. Overall gait planning algorithm.

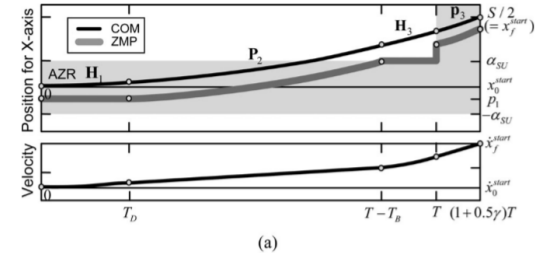


(a)

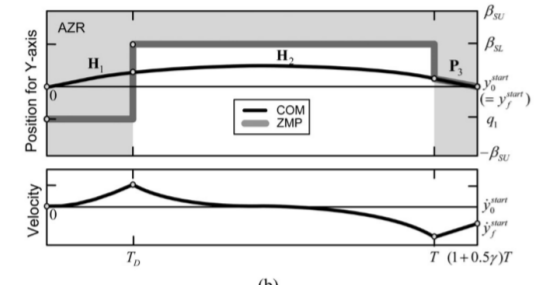


(b)

Fig. 4. Reference COM/ZMP trajectories for the cyclic step. (a) Sagittal motion. (b) Lateral motion.



(a)



(b)

Fig. 5. Reference COM/ZMP trajectories for the starting step. (a) Sagittal motion. (b) Lateral motion.

### 39) An Improved ZMP Trajectory Design for the Biped Robot BHR

[Wei Xu, Q. Huang, Jing Li, Zhangguo Yu, Xuechao Chen and Qian Xu, "An improved ZMP trajectory design for the biped robot BHR," 2011 IEEE International Conference on Robotics and Automation, Shanghai, 2011, pp. 569-574.]

**Robot:** 38 DOF robot

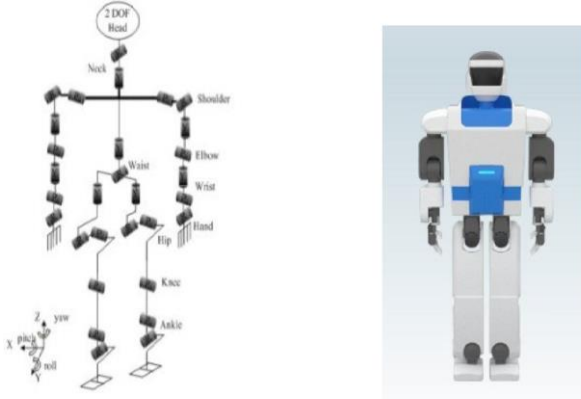


Fig. 4. Appearance of BHR

**Fall Criteria:** ZMP

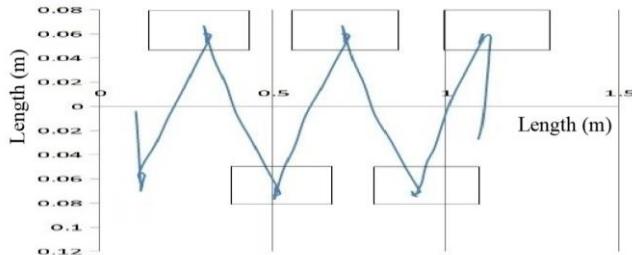


Fig. 6. Traditional ZMP trajectory on the x-y plane

**Threshold:**

**SSP:**

If a robot is in SSP, as is shown in Fig. 8, the stability region moves forward at a speed of V. The calculation process is shown by (7) and (8).

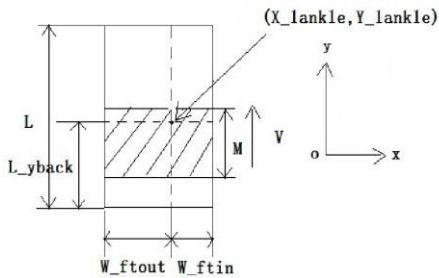


Fig. 8. The movable stability region in SSP

$$\begin{cases} \max_{xzmp} = x_{lankle} + W_{ftin} \\ \min_{xzmp} = x_{lankle} - W_{ftout} \end{cases} \quad (7)$$

$$\begin{cases} \max_{yzmp} = y_{lankle} - L_{yback} + M \\ \quad + V \times t \\ \min_{yzmp} = y_{lankle} - L_{yback} + V \times t \end{cases} \quad (8)$$

DSP: polygon formed by point 0 to point 3

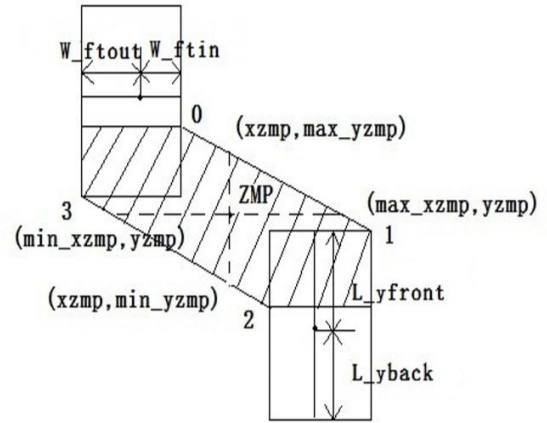


Fig. 9. The changeless stability region in DSP

**Control Policy:**

Hip Strategy

### 40) On-Line Gait Adjustment for Humanoid Robot Robust Walking Based on Divergence Component of Motion

[S. Dong, Z. Yuan, X. Yu, J. Zhang, M. T. Sadiq and F. Zhang, "On-Line Gait Adjustment for Humanoid Robot Robust Walking Based on Divergence Component of Motion," in IEEE Access, vol. 7, pp. 159507-159518, 2019.]

**Robot:** 10 DOF robot

**Fall Criteria:** DCM

**Threshld:**

$$\xi_{\text{plan}} - \xi \geq \text{threshold}$$

**Control Policy:**

Change foot trajectory and step time

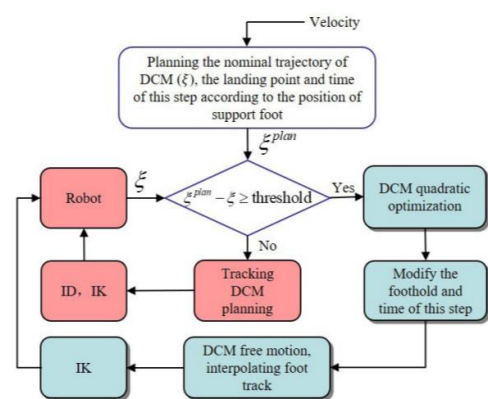


FIGURE 1. Optimal control structure of walking machine.

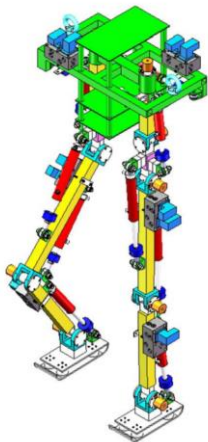
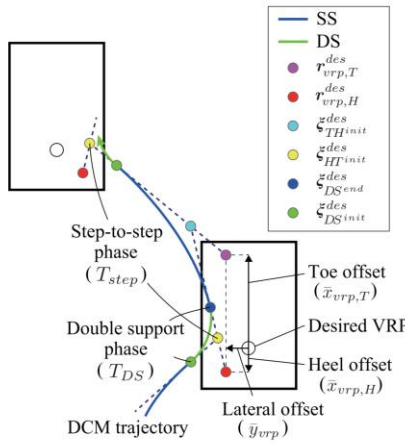


FIGURE 7. The biped robot.

#### 41) The VRP Generalized Inverse and Its Application in DCM/VRP-Based Walking Control

[D. N. Nenchev, A. Miyata, S. Miyahara and T. Hamano, "The VRP Generalized Inverse and Its Application in DCM/VRP-Based Walking Control," in IEEE Robotics and Automation Letters, vol. 4, no. 4, pp. 4595-4602, Oct. 2019.]



**Robot:** General Humanoid

**Fall Criteria:** DCM

**Threshold:**

Footprint

**Control Policy:**

Change foot trajectory

#### 42) Foot and Body Control of Biped Robots to Walk on Irregularly Protruded Uneven Surfaces

[J. H. Park and E. S. Kim, "Foot and Body Control of Biped Robots to Walk on Irregularly Protruded Uneven Surfaces," in IEEE Transactions on Systems, Man, and Cybernetics, Part B (Cybernetics), vol. 39, no. 1, pp. 289-297, Feb. 2009.]

**Robot:** 28 DOF biped

**Fall Criteria:** ZMP

**Threshold:**

Footprint

**Control Policy:**

Foot Rotation

### III. DISSCUSSION

Year	Paper Number
2001	2
2004	3
2005	2
2006	5
2007	3
2008	3
2009	4
2010	1
2011	2
2012	2
2015	1
2016	3
2017	4
2018	2
2019	5
<b>Total</b>	<b>42</b>

Table 1: Number of papers and their publication year

Above table represents the number of papers read from that year of IEEE publication. The year ranges from 2001 to 2019. The most recent once includes the papers with DCM and CoP as fall criteria. The trend of use of fall criteria, its threshold when the fall is detected and control policy for fall avoidance is discussed in the following sessions. It is also observed during the search for the research articles on fall

detection and control of humanoid robots that there is a drastic increase in the study of the field. The availability and the number of articles on the subject of study increases as we come closer to year 2019.

Some important terminologies:

**ZMP:** Zero moment point is a concept related with dynamics and control of legged locomotion, e.g., for humanoid robots. It specifies the point with respect to which dynamic reaction force at the contact of the foot with the ground does not produce any moment in the horizontal direction, i.e. the point where the total of horizontal inertia and gravity forces equals 0 (zero).

**Limit Cycle:** Limit Cycle Walking is a nominally periodic sequence of steps that is stable as a whole but not locally stable at every instant in time.

**DCM:** Some nonlinear control systems admit an exponential dichotomy (Coppel, 1966), that is to say, their dynamics can be decomposed into (exponentially) stable and unstable components. Walking robots fall into this category, and we call their unstable components *divergent components of motion* (DCM).

**CoP:** Center of pressure (CoP) is the term given to the point of application of the ground reaction force vector. The ground reaction force vector represents the sum of all forces acting between a physical object and its supporting surface.

**FRI:** A point which is a point on the foot/ground contact surface where the net ground reaction force would have to act to keep the foot stationary.

Table according to fall criteria

Fall Criteria	Control Policy	Robot
Limit Cycle	Backstepping control	planar compass biped robot
Limit Cycle	Change foot contact location.	Planer biped robot
Limit Cycle	Stepping + design change	Planer compass model
Limit Cycle	Stepping	Prototype Mike
Limit Cycle	CoP and Reflex control	Roboray 32 joint
Limit Cycle	Stepping	7 DOF 3d Biped
Limit Cycle	Change foot contact location.	7 DOF biped
ZMP + IMU	Stepping	T-FloW humanoid
ZMP + COM initial condition	.	LIPM
ZMP	.	8 link Biped
ZMP	Changing swing foot trajectory	DARwIN-OP
ZMP	Hip Strategy	38 DOF
ZMP	Ankle + Hip strategy	NAO H25
ZMP	Stepping + Trunk rotation	GiCeiRA – 2 leg + trunk
ZMP	Ankle + Hip Strategy	6 DOF biped model
ZMP	change in spine motions	Single legged 4 segmented spine robot
ZMP	Ankle + Hip Strategy	3 link model
ZMP	Assist knee	7 DOF biped model
ZMP	Ankle + Hip and Stepping	3 link model
ZMP	Change in Foot trajectory	12 DOF biped Robot
ZMP	Foot Rotation	28 DOF biped
CoP	Ankle Strategy	2 link mode
CoP	Ankle, Hip, Step, Reach & grasp	two-link planar model
CoP	Reflex + Recover using Hip + Knee +Ankle	4 link planer
CoP	Knee, Hip and Ankle strategy	6 DOF biped Robot
CoP	Ankle Strategy	NAO
DCM	Changing Swing leg landing position.	ELIPPFM
DCM	Online Foot Step Adjustment:	LIPM
DCM	Stepping	LIPM
DCM	Ankle Strategy	GAZELLE – 13 DOF
DCM	Change foot trajectory and step time	10 DOF robot
DCM	Change foot trajectory	General Humanoid
CoM -ZRAM	Chaning swing leg trajecotry	7 DOF bipedal Model
FRI	Stepping	General Humanoid
State Classification	Step up leg	6 DOF model
Not Studied	Information about ankle strategy	26DOF humanoid robot

Table 2: Fall Criterias and control policy

The above table refers to the different types of fall criterias used in the papers for different legged robots. Those criterias include Limit Cycle, ZMP, CoP, DCM, CoM, FRI, State classification, etc. Most widely used fall criteria in the papers read is ZMP with 13 papers using the criteria, Limit Cycle with 7 papers using it and DCM and CoP with 6 and 5 papers each. For each fall criteria, different types of control policies are implemented that includes, stepping strategy, Change in foot trajectory, joint trajectories such as Hip, Ankle, Knee strategies, Foot rotation, Trunk Rotation, etc.

Fall Criteria	Number of Papers	Widely used control method	Widely applied Threshold
ZMP	13	Ankle + Hip strategy	Support Polygon
ZMP + CoM initial conditions	1	.	
Limit Cycle	7	Stepping	Boundary condition
DCM	6	Changing foot trajectory	previewed footprint
CoP	5	Ankle + Hip strategy	Footprint
FRI	1	Stepping	
CoM	1	Changing swing leg trajectory	
State Classification	1	Stepping	
Not studied	1	.	
<b>Total</b>	<b>36</b>		

Table 3: Fall criteria study

Above table refers to the number of papers stating the particular fall criteria, widely used control policy and the threshold applied for the fall criteria. It can be observed that the greatest number of papers read are of ZMP fall criteria.

Control Policy	Number of Papers	Widely Used Fall Criteria
Stepping	8	Limit-4, ZMP-2, CoP-2, DCM-1, FRI-1, State-1
Change foot trajectory	8	ZMP-3, DCM-3, Limit-1, CoM-1
Joint strategies	13	ZMP-7, CoP-5, DCM-1
Foot rotation	1	ZMP-1
Stepping + Trunk Rotation	1	ZMP-1
Other	2	
Not studied	3	
<b>Total</b>	<b>36</b>	

Table 4: Control Policy study

Above table refers to the number of papers using a particular control policy and widely used fall criteria for that particular control policy.

Year	Fall Criteria	Control Policy	Robot
2019	CoP	Ankle Strategy	NAO
2019	DCM	Changing Swing leg landing position.	ELIPPFM
2019	DCM	Online Footstep Adjustment:	LIPM
2019	DCM	Ankle Strategy	GAZELLE – 13 DOF
2019	DCM	Change foot trajectory and step time	10 DOF robot
2019	DCM	Change foot trajectory	General Humanoid
2018	ZMP + IMU	Stepping	T-FloW humanoid
2018	ZMP	Ankle + Hip strategy	NAO H25
2017	Limit Cycle	Change foot contact location.	7 DOF biped
2017	ZMP + COM initial condition	.	LIPM
2017	CoP	Ankle, Hip, Step, Reach & grasp	two-link planar model
2017	CoM -ZRAM	Changing swing leg trajectory	7 DOF bipedal Model
2016	Limit Cycle	Backstepping control	planar compass biped robot
2016	DCM	Stepping	LIPM
2015	ZMP	Changing swing foot trajectory	DARwIN-OP
2015	ZMP	Stepping + Trunk rotation	GiCeIRA – 2 leg + trunk
2012	Limit Cycle	CoP and Reflex control	Roboray 32 joint
2011	ZMP	Hip Strategy	38 DOF
2011	CoP	Knee, Hip and Ankle strategy	6 DOF biped Robot
2010	Limit Cycle	Stepping + design change	Planer compass model
2010	Limit Cycle	Stepping	7 DOF 3d Biped
2009	Limit Cycle	Change foot contact location.	Planer biped robot
2009	ZMP	Ankle + Hip and Stepping	3 link model
2009	ZMP	Foot Rotation	28 DOF biped
2008	ZMP	Ankle + Hip Strategy	3 link model
2008	State Classification	Step up leg	6 DOF model
2007	ZMP	Ankle + Hip Strategy	6 DOF biped model
2007	CoP	Ankle Strategy	2 link mode
2006	ZMP	.	8 link Biped
2005	Limit Cycle	Stepping	Prototype Mike
2005	CoP	Reflex + Recover using Hip + Knee +Ankle	4 link planer
2004	ZMP	change in spine motions	Single legged 4 segmented spine robot
2004	ZMP	Assist knee	7 DOF biped model
2004	FRI	Stepping	General Humanoid
2001	ZMP	Change in Foot trajectory	12 DOF biped Robot
2001	Not Studied	Information about ankle strategy	26DOF humanoid robot

Table 5: Study of fall criteria and control policy according to year

One of the main observations that can be made using this table is that mostly DCM has been used in the papers that were published in 2019 and that were read by me.

**IV. ACKNOWLEDGEMENT**

This project is done under the guidance of Professor J.H. Kim. I would like to express our sincere gratitude to Professor Kim for providing his invaluable guidance, comments and suggestions throughout the course of the project. I would also thank our classmates for their questions, comments and suggestions.